MOLECULAR AND CELLULAR BIOLOGY, Jan. 2007, p. 324–339 Vol. 27, No. 1
0270-7306/07/$08.00+0 doi:10.1128/MCB.01394-06

Dual Role of SnoN in Mammalian Tumorigenesis▽

Qingwei Zhu,[1,2] Ariel R. Krakowski,[1] Elizabeth E. Dunham,[1] Long Wang,[3] Abhik Bandyopadhyay,[3] Rebecca Berdeaux,[1] G. Steven Martin,[1,2] LuZhe Sun,[3] and Kunxin Luo[1,2]*

Department of Molecular and Cell Biology, University of California, Berkeley,[1] and Life Sciences Division, Lawrence Berkeley National Laboratory,[2] Berkeley, California 94720, and Department of Cellular and Structural Biology, University of Texas Health Science Center, San Antonio, Texas 78229-3900[3]

Received 28 July 2006/Returned for modification 19 September 2006/Accepted 16 October 2006

SnoN is an important negative regulator of transforming growth factor β signaling through its ability to interact with and repress the activity of Smad proteins. It was originally identified as an oncoprotein based on its ability to induce anchorage-independent growth in chicken embryo fibroblasts. However, the roles of SnoN in mammalian epithelial carcinogenesis have not been well defined. Here we show for the first time that SnoN plays an important but complex role in human cancer. SnoN expression is highly elevated in many human cancer cell lines, and this high level of SnoN promotes mitogenic transformation of breast and lung cancer cell lines in vitro and tumor growth in vivo, consistent with its proposed prooncogenic role. However, this high level of SnoN expression also inhibits epithelial-to-mesenchymal transdifferentiation. Breast and lung cancer cells expressing the shRNA for SnoN exhibited an increase in cell motility, actin stress fiber formation, metalloprotease activity, and extracellular matrix production as well as a reduction in adherens junction proteins. Supporting this observation, in an in vivo breast cancer metastasis model, reducing SnoN expression was found to moderately enhance metastasis of human breast cancer cells to bone and lung. Thus, SnoN plays both protumorigenic and antitumorigenic roles at different stages of mammalian malignant progression. The growth-promoting activity of SnoN appears to require its ability to bind to and repress the Smad proteins, while the antitumorigenic activity can be mediated by both Smad-dependent and Smad-independent pathways and requires the activity of small GTPase RhoA. Our study has established the importance of SnoN in mammalian epithelial carcinogenesis and revealed a novel aspect of SnoN function in malignant progression.

SnoN is a member of the Ski family of proto-oncogenes that was originally identified based on sequence homology with v-Ski, the transforming protein of the Sloan Kettering virus (42, 44, 45). It has been classified as a proto-oncoprotein since its initial characterization, based largely on its ability to induce anchorage-independent growth of chicken and quail embryo fibroblasts when overexpressed (12). Whether and how SnoN affects mammalian carcinogenesis has not been well understood. Consistent with its role as an oncoprotein, elevated SnoN expression has been observed in human carcinoma cells of the lung, breast, vulva, stomach, ovary, and thyroid (32, 42, 67). The increase in SnoN expression observed in human cancer cells can occur by one of several mechanisms, including gene amplification, transcriptional activation, and increased protein stability (11, 24, 32, 55, 56, 68). However, it appears that SnoN can also act as a negative regulator of tumor progression. Deletion of one copy of the *sno* gene resulted in increased susceptibility to carcinogen-induced tumor formation, suggesting that SnoN may also possess tumor-suppressive as well as oncogenic activities (53). Moreover, SnoN was recently shown to cooperate with p53 in the silencing of the alpha fetoprotein gene, which is aberrantly overexpressed postnatally in liver cancer cells (62). These data support a dual role for SnoN in the regulation of tumorigenesis. However, the tumor-promoting and tumor-suppressive activities of SnoN have not previously been reconciled in a model of cellular transformation, and the mechanism by which SnoN regulates malignant progression has not been characterized.

SnoN has been shown to be an important negative regulator of transforming growth factor β (TGF-β) signaling (56, 58). TGF-β plays a complex and multifaceted role in the regulation of tumorigenesis (2, 54, 61). On the one hand, TGF-β induces cell cycle arrest or apoptosis in many cell types, and therefore acts as a potent inhibitor of cell proliferation. These antimitogenic responses to TGF-β are frequently lost early in malignant transformation, and the remaining effects of TGF-β on tumor cells and their surrounding microenvironment promote malignant progression. The ability of TGF-β to induce epithelial-to-mesenchymal transition (EMT) plays a critical role in the acquisition of a migratory, invasive phenotype that is correlated with enhanced metastatic potential in tumor cells. Whereas the signal transduction pathways leading to TGF-β-induced EMT have not been fully characterized, the mechanism by which TGF-β elicits growth arrest has been elucidated. The Smad proteins are critical mediators of cytostatic responses to TGF-β. Upon ligand binding, the activated TGF-β receptor kinase complex phosphorylates the receptor-associated Smads (R-Smads), Smad2 and Smad3, leading to their hetero-oligomerization with Smad4 and the accumulation of Smad complexes in the nucleus, where they interact with other transcription factors to regulate expression of TGF-β-responsive genes (4, 23, 40, 41).

We and others have shown that SnoN interacts directly with Smad2, Smad3, and Smad4 and represses their ability to activate expression of TGF-β target genes by disrupting the for-

* Corresponding author. Mailing address: Dept. of Molecular and Cell Biology, University of California, Berkeley, 16 Barker Hall, Mail code 3204, Berkeley, CA 94720-3204. Phone: (510) 643-3183. Fax: (510) 643-6334. E-mail: kluo@berkeley.edu.

▽ Published ahead of print on 30 October 2006.

mation of an active heteromeric Smad complex, recruiting a transcriptional corepressor complex, and by blocking the interaction of transcriptional coactivators with Smad2 and Smad3 (3, 38, 56, 63). When localized to the cytoplasm, SnoN antagonizes TGF-β signaling by sequestering Smad proteins in the cytoplasm (36). The transforming activity of SnoN may be dependent on its ability to bind to Smad proteins, since Smad binding was shown to be required for repression of TGF-β-induced growth arrest as well as oncogenic transformation of chicken embryo fibroblasts (29). In addition to the Smad proteins, SnoN has also been shown to interact with other transcription factors, including nuclear hormone receptor corepressor N-CoR/SMRT, mSin3A, methyl-CpG-binding protein MeCP2, and TAF(II)110 (16, 35, 53), to mediate transcriptional repression. However, it is not clear whether these interactions involve Smad proteins or occur independently of them. It is also not clear whether any of these interactions is required for the transforming activity of SnoN.

In this study, we investigated the role of SnoN in tumorigenesis by ablating its expression in two different human cancer cell lines that exhibit elevated expression of SnoN. We show that reducing SnoN expression inhibits the proliferative potential of cancer cells both in vitro and in vivo but promotes EMT and tumor metastasis. Thus, SnoN exerts opposite effects at different stages of tumorigenesis. In addition, we have also attempted to explore the signaling molecules and downstream effectors associated with these SnoN activities. We find that both Smad-dependent and Smad-independent pathways are involved in the activities of SnoN during tumorigenesis.

MATERIALS AND METHODS

Cell culture and DNA constructs. The A549 lung adenocarcinoma cell line was maintained in F-12K nutrient mixture (Kaighn's modification) supplemented with 10% fetal bovine serum (FBS). MDA-MB-231 and MDA-MB-435 breast cancer cell lines were cultured in Dulbecco's modified Eagle's medium (DMEM) containing 5% FBS. MCF7 breast cancer cells, A375 melanoma cells, and SW1271 lung cancer cells were maintained in DMEM supplemented with 5% FBS. ZR75b human breast cancer cells were cultured in DMEM-F12 medium containing 10% FBS. A427 lung carcinoma cells and HT-1080 fibrosarcoma cells were propagated in minimal essential medium containing 10% FBS. The human rhabdomyosarcoma A-204 cell line was cultured in McCoy's medium supplemented with 10% FBS. All of the above-listed human cancer cell lines were purchased from ATCC. Normal human mammary epithelial cell lines HMT3522-S1 and MCF10A were generous gifts of M. J. Bissell and were maintained as described elsewhere (13, 20).

A small hairpin RNA (shRNA) vector targeting human SnoN was generated using the pSUPER vector system as described previously (14). Oligonucleotide pairs encoding shRNA against human SnoN were designed according to established guidelines using Oligoengine software. The 19-nucleotide sequence within SnoN targeted by the shRNA oligonucleotide pair was 5′-GACAGTCAGAGA AGGCTCA-3′ at nucleotide position number 1307 within the human SnoN cDNA. Forward and reverse primers were synthesized containing this sequence in sense and antisense orientations with an intervening linker. Primer pairs were designed to generate single-strand overhangs upon annealing that would allow the annealed duplex oligonucleotide to be cloned into BglII and HindIII sites in the pSUPER.retro.puro vector. Forward and reverse primers were annealed and ligated into the pSUPER.retro.puro vector.

Smad-binding mutant SnoN construct was generated as described previously (29, 63). pGEX-2T-TRBD was obtained from M. Schwartz. pGEX-2T-PBD was obtained from G. Bokoch.

Transfections and generation of stable cell lines. All transfections were performed using the Lipofectamine Plus transfection system (Invitrogen) according to the manufacturer's instructions. MDA-MB-231 breast cancer and A549 lung cancer cell lines that stably express shRNA constructs targeting human SnoN were generated by cotransfecting each cell line with the pSUPER-shSnoN vector along with the pBABE puro vector to permit selection using puromycin resistance. At 48 h posttransfection, stably transfected cells were selected by culture in medium containing 1.5 μg/ml puromycin. For "rescue" experiments, wild-type or Smad-binding mutant SnoN constructs were constructed containing nonsense mutations within the sequence targeted by shSnoN and therefore were not recognized by the shRNA. These SnoN constructs were cotransfected into shSnoN A549 cells along with the pLXSN neomycin resistance vector. Transfected cells were selected by growth in medium containing 0.8 mg/ml neomycin (Invitrogen).

Cell lysis, immunoprecipitation, and immunoblotting. Cells were lysed in high-salt lysis buffer (420 mM NaCl, 50 mM HEPES-KOH, pH 7.8, 5 mM EDTA, 0.1% NP-40, 3 mM dithiothreitol, 0.5 mM phenylmethylsulfonyl fluoride [PMSF], 10 μg/ml aprotinin). Prior to immunoprecipitation, cell lysates were precleared on 30 μl of protein A-Sepharose beads for 30 min at 4°C. Precleared lysates were then transferred to beads complexed with the appropriate antibody for immunoprecipitation. Endogenous SnoN was immunoprecipitated using protein A-Sepharose beads coupled to a polyclonal antibody recognizing a C-terminal SnoN peptide (KELKLQILKSSKTAKE). Endogenous Ski was immunoprecipitated using a polyclonal anti-Ski antibody raised against a glutathione *S*-transferase (GST)–fusion protein containing amino acid residues 1 to 605 of human c-Ski.

Antibodies used for immunoblotting were anti-Ski (G8; Cascade Bioscience), anti-SnoN (H-317; Santa Cruz Biotechnology), anti-Smad2 (BD Transduction Labs), anti-Smad3 (FL-425; Santa Cruz Biotechnology), anti-cofilin (Sigma), anti-phospho-cofilin (Cell Signaling), anti-E-cadherin (BD Transduction Laboratories), anti-fibronectin (BD Transduction Laboratories), anti-RhoA (Santa Cruz Biotechnology), anti-Rac1 (Upstate), and anti-Cdc42 (Santa Cruz Biotechnology). Anti-phospho-Smad2 and anti-phospho-Smad3 antibodies were kind gifts of A. Moustakis (Ludwig Institute for Cancer Research, Uppsala, Sweden).

Growth inhibition assay. A total of 3×10^4 MDA-MB-231 cells or 5×10^4 A549 cells were cultured with the indicated concentrations of TGF-β1 for 4 days. Relative cell growth was determined by counting cells and calculating the number of TGF-β-treated cells relative to that of unstimulated cells.

Immunofluorescence. For actin stress fiber staining, cells were cultured in medium containing 1% serum on glass coverslips for 20 h prior to treatment with 50 pM TGF-β1 for another 3 days before staining. Cells were fixed in 4% paraformaldehyde in phosphate-buffered saline (PBS) for 20 min, and the paraformaldehyde was quenched with three washes in 100 mM glycine in PBS. Cells were permeabilized in 0.1% Triton X-100, and actin filaments were stained with rhodamine-phalloidin (Molecular Probes) for 30 min at room temperature. Coverslips were then washed three times for 5 min each in PBS before being mounted on slides in one drop of mounting medium, consisting of 80% glycerol, 20 mM Tris, pH 8.0, and 1:1,000 DABCO [1,4-diazabicyclo-(2,2,2)-octane; Sigma].

To visualize transfected Myc-RhoA T19N, coverslips were blocked for 1 h following the permeabilization step in blocking buffer (PBS containing 10% newborn calf serum, 1% bovine serum albumin, and 0.02% Triton X-100). After blocking, coverslips were incubated with anti-Myc antibody (Sigma) in staining buffer (blocking buffer lacking bovine serum albumin) overnight at 4°C. Coverslips were washed three times in staining buffer and then incubated with Alexa 488-conjugated anti-mouse antibody (Molecular Probes) for 1 h at room temperature. Coverslips were then washed three times in PBS before being mounted on slides in one drop of mounting medium. For E-cadherin staining, cells were grown until reaching 90% confluence and then fixed in 50/50 methanol-acetone for 10 min at −20°C. Anti-E-cadherin antibody was purchased from Transduction Laboratories.

Immunofluorescence was observed with a Zeiss Axiophot epifluorescence microscope or a Zeiss confocal LSM 510 microscope.

Semiquantitative reverse transcription-PCR (RT-PCR). Total RNA from parental A549 and MDA-MB-231 cells and their shSnoN-expressing derivatives was extracted using the RNeasy mini kit (QIAGEN) and treated with RNase-free DNase (QIAGEN). cDNA was produced using reverse transcriptase (SuperScript II; Invitrogen) and was amplified with the following sets of primers: *GAPDH*, 5′-CGTCTTCACCACCATGGAGA-3′ (forward) and 5′-CGGCCAT CACGCCACAGTTT-3′ (reverse); *EMP1*, 5′-GGTTAGAGAGATTGGCCAG C-3′ (forward) and 5′-CAGTACTAGAACAATCCACC-3′ (reverse); *PLAU*, 5′-AGCAGCTGAGGRCTCTTGAG-3′ (forward) and 5′-AAACTGAGACAG TGCTGGTC-3′ (reverse); *Twist1*, 5′-GAAAGCGAGACAGGCCCGTG-3′ (forward) and 5′-GATTGGCACGACCTCTTGAG-3′ (reverse); EGFR, 5′-TG TCTCTGCCTTGAGRCATC-3′ (forward) and 5′-ACTGCTGTTAACCAGTC AGG-3′ (reverse); *VEGF*, 5′-GGGCAACTTGTATTTGTGTG-3′ (forward) and 5′-CTGCACTAGAGACAAAGACG-3′ (reverse); *JunB*, 5′-ACGTCAGC AACGGCTGTCAG-3′ (forward) and 5′-GAATCGAGTCTGTTTCCAGC-3′

(reverse); *GADD45A*, 5′-CTGAACGGTGATGGCATCTG-3′ (forward) and 5′-GCAAAGTCATCTATCTCCGG-3′ (reverse).

EMP1, *PLAU*, *Twist1*, *EGFR*, *VEGF*, *JunB*, and *GADD45A* mRNA levels were determined by semiquantitative PCR. *GAPDH* served as an internal control. The following PCR program was performed: 94°C for 5 min (initial denaturation) and 94°C for 30 s, 55°C for 30 s, and 72°C for 45 s. Within the linear range of amplification, all of the PCR products were prepared under appropriate cycling conditions and separated on a 1% agarose gel. The band densities were compared between samples from parental and shSnoN-expressing cells.

Northern blotting. Prior to RNA extraction, MDA-MB-231 cells or A549 cells were starved in medium containing 0.1% FBS overnight, and parallel dishes were treated with 100 pM TGF-β for the times indicated. Total RNA was extracted using the RNeasy mini kit (QIAGEN). Twenty micrograms of RNA was resolved on a 1% formaldehyde gel, transferred to a nylon membrane, and analyzed by Northern blotting. DNA probes for p21 and PAI-1 were radiolabeled by random priming (Stratagene) and hybridized with the nylon membrane in QuikHyb (Stratagene).

Microarray hybridization, data collection, and analysis. Affymetrix human genome U133 A+B GeneChips were used in this study. Fifteen micrograms of total RNA collected from parental and shSnoN-expressing A549 cells was used for microarray probe synthesis as described in the Affymetrix GeneChip manual. Microarray hybridization, data collection, and analysis were performed by the Stanford PAN facility. The gene expression profiles were compared between parental and shSnoN-expressing samples. The parental samples were used as the "baseline." The expression pattern of genes was considered changed in shSnoN cells only when two statistical analysis criteria were satisfied: (i) a probe set with a detection *P* value that was less than 0.4, which is considered PRESENT by the Affymetrix GeneChip program, and (ii) the change in gene expression between the experimental (shSnoN sample) and baseline (parental sample) conditions was greater than 1.75-fold. The signal log ratio is related to the change (*n*-fold) by the following formulas: change (*n*-fold increase) = $2^{\text{signal log ratio}}$ for signal log ratios of ≥0; change (*n*-fold decrease) = $(-1) \times 2^{\text{signal log ratio}}$ for signal log ratios of <0.

Selected microarray results were verified by Northern blotting analysis, semiquantitative RT-PCR, and immunoblotting.

Wound healing assay. A549, MDA-MB 231, or their derivative cell lines were seeded into six-well dishes and grew until 90% confluence. One-milliliter plastic tips were used to generate wounding across the cell monolayer. Phase contrast pictures were taken under an inverted microscope at the time of wounding (0 h) and 48 h later. The wound closure was estimated as the percentage of the closure area to the initial wounded area. Experiments were carried out in triplicate at least three times.

Rho/Rac/Cdc42 GTPase assays. The protocol for measuring GTP loading on Rho family GTPases was as described previously (8). The GST fusion construct used to bind Rho-GTP was pGEX-2T-TRBD, which contains the Rho-binding domain of rhotekin corresponding to amino acids 7 to 89. The GST fusion construct used to bind Rac-GTP or Cdc42-GTP was pGEX-2T-PBD. GST fusion proteins were expressed in DH5α *Escherichia coli* bacteria and purified using glutathione-Sepharose beads (Amersham). After washing to remove unbound protein, the beads were resuspended in wash buffer containing 10% glycerol and assayed for protein concentration before being stored at −80°C.

To prepare cell lysates, A549 cells or MDA-MB-231 cells were washed in ice-cold Tris-buffered saline and lysed in RIPA buffer (50 mM Tris, pH 7.2, 1% Triton X-100, 0.5% sodium deoxycholate, 0.1% sodium dodecyl sulfate, 500 mM NaCl, 10 mM $MgCl_2$, 5 μg/ml each of leupeptin and aprotinin, and 1 mM PMSF). Lysates were clarified by centrifugation at 13,000 × *g* at 4°C for 5 min, and protein concentration was measured for all samples. For determination of RhoA-GTP loading, 700 μg of whole-cell lysate in a 500-μl total volume was incubated with 60 μg of GST-TRBD beads. For determination of Rac-GTP or Cdc42-GTP binding, 500 μg of whole-cell lysate in a 400-μl total volume was incubated with 30 μg of GST-PBD beads. Lysates were incubated with beads for 1 h at 4°C with constant rotation and subsequently washed three times with wash buffer (50 mM Tris, pH 7.2, 1% Triton X-100, 150 mM NaCl, 10 mM $MgCl_2$, 5 μg/ml each of leupeptin and aprotinin, and 0.1 mM PMSF). The beads were resuspended in 20 ml of 2× sample buffer containing dithiothreitol and heated at 95°C for 10 min. The samples were run on a 12% polyacrylamide gel electrophoresis gel and transferred to a nitrocellulose membrane. Bound Rho proteins were detected by immunoblotting using either anti-RhoA (Santa Cruz Biotechnology), anti-Rac1 (Upstate), or anti-Cdc42 (Santa Cruz Biotechnology) antibody. A small sample of each cleared lysate was reserved for analysis of total Rho protein present in the original sample.

In situ zymography. Glass coverslips were coated with a thin layer of Alexa 488-conjugated gelatin (0.2 mg/ml in 2% sucrose–PBS). The coated coverslips were fixed with cold 0.5% glutaraldehyde in PBS for 15 min and incubated for 3 min in 5 mg/ml $NaBH_4$ at room temperature. The coverslips were then sterilized with 70% ethanol, washed three times in PBS, and quenched with serum-free DMEM for 1 h at 37°C. Cells were plated on coated coverslips in complete medium. After the cells had attached, the medium was aspirated, and the cells were incubated in DMEM containing 0.1% FBS with or without either 100 pM TGF-β1 alone or in the combination with 10 μM matrix metalloprotease (MMP) inhibitor GM6001 for 24 h (in breast cancer cells) or 48 h (in lung cancer cells) before being processed for immunostaining.

Soft agar assay. A concentrated bottom layer comprised of 2 ml of growth medium containing 0.66% Bacto-agar (Difco) was poured into a six-well dish. A total of 5×10^3 A549 cells, MDA-MB 231 cells, or their shSnoN-expressing derivatives were resuspended in 2 ml of medium containing 0.4% agar and overlaid on the hardened bottom layer. One milliliter of fresh medium containing 0.4% agar was added to the dish every week. After 4 weeks of incubation, colonies were visualized by staining with 0.5 mg/ml thiazolyl blue tetrazolium bromide (MTT; Sigma) and scanned on a Hewlett-Packard ScanJet 5500C to visualize the colonies.

Tumorigenicity in nude mice. Female athymic BALB/c mice were supplied by Charles River Laboratories at 4 to 6 weeks of age. A549 cells, MDA-MB-231 cells, or their shSnoN-expressing derivatives were injected subcutaneously into the left and right flanks of nude mice. To prepare cells for injection, cells were trypsinized and resuspended in medium containing 10% FBS to neutralize the trypsin. The cell pellets were then washed twice in PBS and resuspended in PBS at a concentration of 5×10^6 cells/0.1 ml PBS (A549) or 2×10^6 cells/0.1 ml PBS (MDA-MB 231). A 0.1-ml aliquot of the cell suspension was injected into each injection site using a 26-gauge needle with a 1-ml sterile syringe. Tumor growth was monitored once a week. Mice were sacrificed at 8 weeks after injection, and tumors were surgically isolated. Tumor volume (*V*) was calculated by using the formula: $V = \text{length} \times \text{width} \times \text{thickness}$.

Metastasis assays. MDA-MB-231 cells (1×10^5 cells in 0.1 ml PBS/mouse) were injected into the left cardiac ventricle of 4-week-old female nude mice. The body weight of each mouse was measured weekly. Animals were monitored for paraplegia and were terminated at the end of 4 weeks after the injection at the sign of paraplegia of some animals. After the mice were sacrificed, whole lungs were excised and fixed with Bouin's solution. Metastatic nodules were identified by color and appearance and counted under a dissecting microscope. The right tibia and femur bones were fixed in buffered formalin and used for histomorphometry analyses.

To detect paraplegia as a measure of metastatic body burden, a wire hang test was employed (28). Each mouse was placed on a wire cage lid. The lid was inverted, and the latency to fall was recorded, with a 60-second cutoff time. The results were plotted as mean latency to fall in seconds ± the standard error of the mean (SEM).

To examine metastasis of A549 lung cancer cells, 2×10^6 parental or shSnoN-expressing cells in 0.1 ml PBS were injected into the lateral tail veins of 4-week-old female nude mice. The body weight of each mouse was taken every week. After 3 months, the mice were sacrificed. Lungs were excised and fixed in Bouin's solution. Metastasis nodules showed a different color from that of lung tissue and were counted.

RESULTS

Expression of SnoN is elevated in human cancer cells. To understand the contribution of SnoN and Ski to epithelial cell transformation, we first examined their expression levels in a number of cell lines derived from different types of human cancer. These included human breast cancer cell lines (MDA-MB-231, MDA-MB-435, and ZR75b), lung adenocarcinoma lines (A427, A549, and SW1271), melanoma (A375), and osteosarcoma (HT1080). Two untransformed human mammary epithelial cell lines, HMT3522-S1 and MCF10A, were included as normal controls. Endogenous SnoN and Ski proteins were isolated by immunoprecipitation from these cell lines, and their expression was detected by immunoblotting with anti-SnoN and anti-Ski antisera, respectively. The level of SnoN protein was strongly elevated in all cancer lines examined compared to untransformed cells, which express low or undetectable levels of SnoN (Fig. 1A). This upregulation of SnoN is

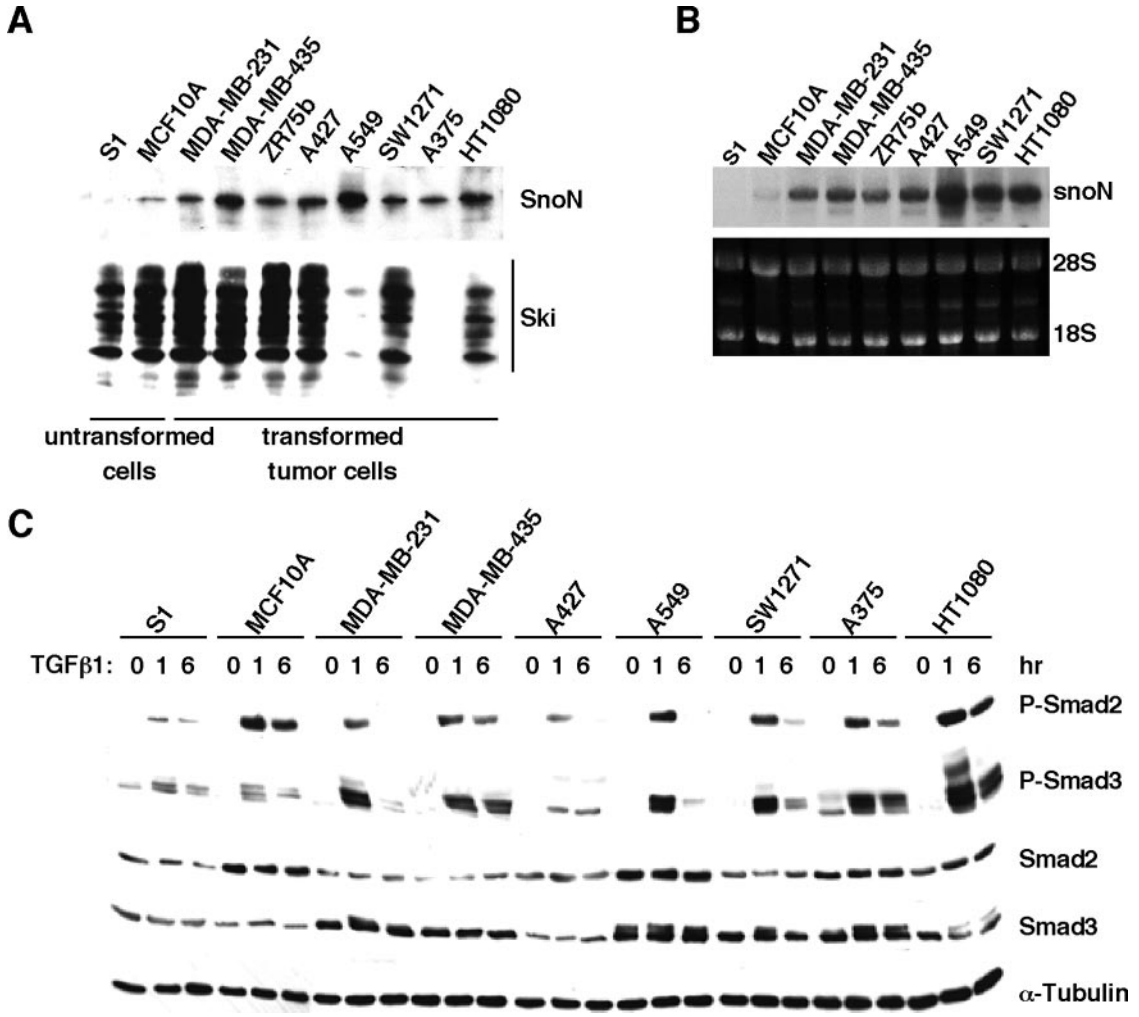

FIG. 1. Expression of SnoN is elevated in human cancer cell lines. (A) Expression levels of SnoN and Ski are regulated differently in human cancer cell lines. Endogenous SnoN or Ski was isolated by immunoprecipitation from equal amounts of cell lysates prepared from the following cell lines: human breast cancer cell lines (MDA-MB-231, MDA-MB-435, and ZR75b), lung adenocarcinoma lines (A427, A549, and SW1271), melanoma (A375), osteosarcoma (HT1080), and two untransformed human mammary epithelial cell lines (HMT3522-S1 and MCF10A). Immune complexes were analyzed by Western blotting with anti-SnoN or anti-Ski. (B) The *snoN* mRNA is upregulated in some cancer cell lines. Twenty micrograms of total RNA was isolated from cancer cell lines described in panel A, and *snoN* expression was analyzed by Northern blotting. 28S and 18S RNA are shown as loading controls. (C) TGF-β-induced phosphorylation of Smad2 and Smad3 in cancer cell lines. Cells were serum starved for 16 h and treated with 100 pM TGF-β1 for the indicated period of time. Equal amounts of total cell lysates were analyzed by Western blotting using antibodies against phospho-Smad2, phospho-Smad3 (P-Smad2 and P-Smad3; top two panels), Smad2 and Smad3 (middle panels), or α-tubulin as a loading control (bottom panel).

mostly due to an increase in *snoN* mRNA (Fig. 1B and data not shown). In addition, no mutations were detected in endogenous SnoN isolated from some of the cancer cell lines. In contrast, the related Ski protein was detected readily in nontumorigenic cell lines, and its expression was barely detectable in some human cancer cell lines, particularly the A549 lung adenocarcinoma and A375 melanoma cells. No significant correlation was observed between SnoN or Ski expression and the intensity and duration of TGF-β-induced phosphorylation of Smad2 and Smad3 (Fig. 1C), consistent with the notion that SnoN and Ski function downstream of Smad phosphorylation.

Thus, the expression of SnoN and Ski appears to be regulated differently during malignant progression. Since SnoN expression is elevated in all cancer cell lines we surveyed, we decided to focus on the role of SnoN in various aspects of mammalian tumorigenesis in this study.

Downregulation of SnoN expression restores TGF-β responses. We chose two model systems, the A549 human lung adenocarcinoma cell line and the MDA-MB-231 human breast cancer cell line, to investigate the role of SnoN in malignant progression. A549 cells express high levels of SnoN but have very little if any Ski (Fig. 1A). MDA-MB-231 cells are derived from invasive and metastatic breast adenocarcinoma and express both SnoN and Ski at high levels. These cell lines are weakly or nonresponsive to TGF-β-induced growth inhibition and, in addition to various aspects of morphological and mitogenic transformation, are also capable of undergoing or have undergone at least some aspects of EMT, an important process

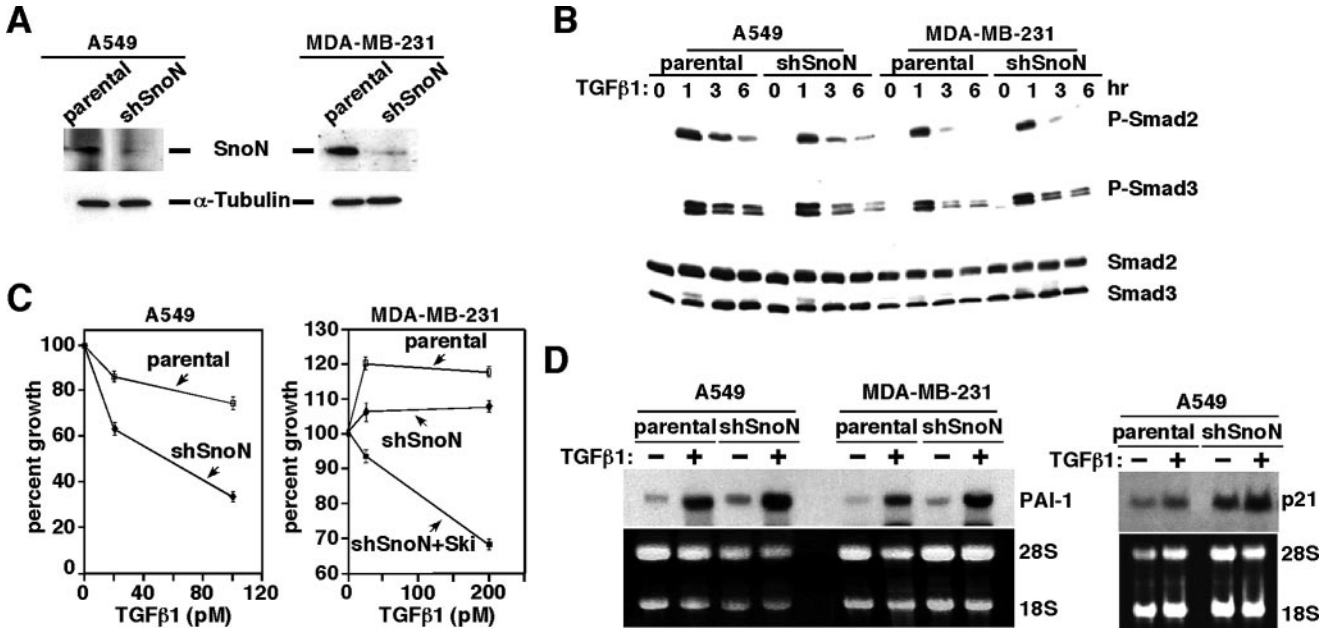

FIG. 2. Reduction of SnoN expression restores TGF-β responses in A549 and MDA-MB-231 cancer cell lines. (A) Reduction of *snoN* expression in A549 lung cancer cells and MDA-MB-231 breast cancer cells by shRNA. Stable shSnoN cell lines expressing the shRNA for human *snoN* were generated as described in Materials and Methods. SnoN expression in the representative stable clones was assessed by immunoprecipitation and Western blotting and compared with that in parental cells. The levels of α-tubulin in cell lysates were measured by Western blotting and included as a loading control. (B) Phosphorylation of R-Smads in response to TGF-β in A549 and MDA-MB-231 parental and shSnoN cell lines. Cells were treated with 100 pM TGF-β1 for the indicated time periods. Equal amounts of total cell lysates were analyzed by Western blotting using antibodies against phospho-Smad2 (P-Smad2; top panel), phospho-Smad3 (P-Smad3; middle panel) or total Smad2 and Smad3 (bottom panel). (C) Effects of TGF-β on the growth of parental cancer cells and their derived shSnoN cells. Parental A549 cells, MDA-MB-231 cells, or their shRNA-expressing derivatives were treated with increasing concentrations of TGF-β1 and cultured for 4 days. The growth of cells was determined by cell counting, and the number is expressed as a percentage of the number of cells in unstimulated samples. (D) SnoN-deficient cells exhibit increased expression of TGF-β-responsive genes. Parental A549 cells, MDA-MB-231 cells, and their shSnoN derivatives were serum starved for 16 h and stimulated with 100 pM TGF-β1 for 3 h. Total RNA was isolated from these cells, and expression of *PAI-1* and *p21* was assessed by Northern blotting. 28S and 18S RNA were included as loading controls.

in later stages of tumorigenesis that may be necessary for tumor invasiveness and metastasis. The multiple features of tumorigenesis exhibited by these cell lines provide an opportunity to probe the contribution of SnoN to various aspects of epithelial transformation. In addition, the different tissue origins of the two cell lines allow us to determine whether the processes affected by SnoN are tissue specific or are common to epithelial tumors.

We generated stable A549 and MDA-MB-231 cell lines in which expression of SnoN was reduced using shRNA specific for human *snoN*. pSUPER vector expressing *snoN* shRNA was introduced into A549 and MDA-MB-231 cells by transfection together with a plasmid expressing a puromycin resistance gene. For each cell line, multiple stable clones were generated that exhibited reduced expression of SnoN (Fig. 2A). Stable reduction of SnoN expression had no effect on the intensity or duration of TGF-β-induced phosphorylation of Smad2 or Smad3, as expected given that SnoN plays no direct role in the regulation of Smad phosphorylation (Fig. 2B).

We have shown previously that SnoN represses TGF-β signaling (56). Therefore, reducing SnoN expression in these TGF-β-unresponsive cancer cell lines might relieve this repression and restore TGF-β signaling. Indeed, in a growth inhibition assay, while the parental A549 cell line was only weakly responsive to TGF-β, cells expressing shSnoN showed a markedly enhanced response to TGF-β-induced growth inhibition (Fig. 2C, left panel). MDA-MB-231 cells have completely lost any growth arrest response to TGF-β and instead proliferate in the presence of TGF-β (Fig. 2C, right panel). Reducing SnoN expression blocked this increased proliferation but did not inhibit the growth of MDA-MB-231 cells (Fig. 2C, right panel). Interestingly, reduction of both SnoN and Ski expression in MDA-MB-231 cells permitted a moderate growth arrest response, with 32% growth inhibition occurring at 200 pM TGF-β, suggesting that the high level of Ski expression in MDA-MB-231 cells may also contribute to the repression of TGF-β-elicited growth arrest.

We next examined whether reducing SnoN expression augmented activation of endogenous TGF-β target gene expression (Fig. 2D). In parental A549 and MDA-MB-231 cells, TGF-β induced expression of PAI-1 mRNA after 3 h of treatment (Fig. 2D, left panel). This induction of PAI-1 by TGF-β was enhanced in both A549 and MDA-MB-231 cells expressing *snoN* shRNA (Fig. 2D, left panel). Likewise, the expression of $p21^{CIP1}$, another TGF-β-inducible gene, was elevated in shSnoN A549 cells even in the absence of TGF-β treatment and further enhanced by TGF-β stimulation (Fig. 2D, right panel). This elevation in basal-level p21 expression in shSnoN A549 cells is not due to the increased autocrine TGF-β activity in these cells, because inhibition of TβRI activity by an inhib-

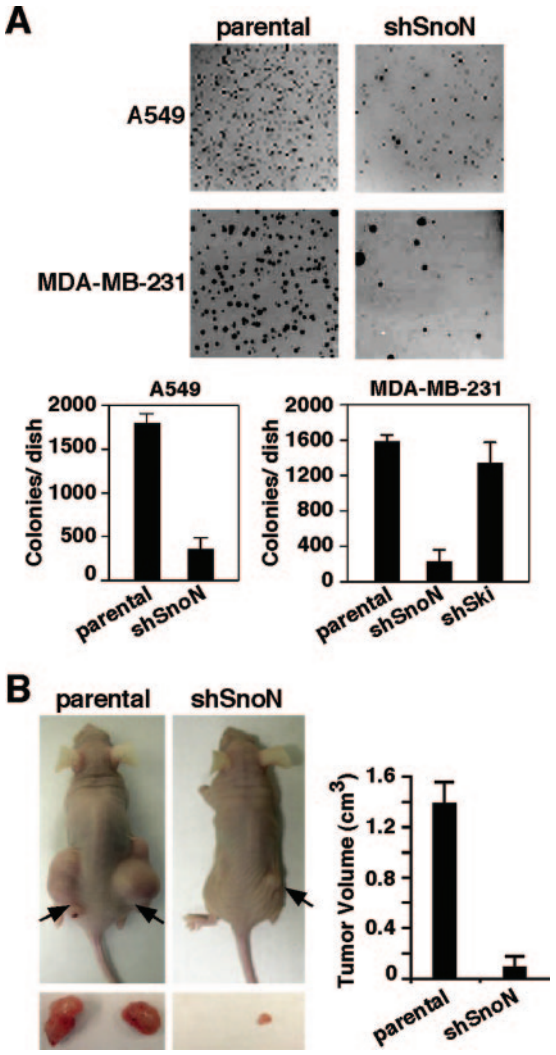

FIG. 3. Reducing SnoN expression suppresses the transformed phenotype of cancer cells. (A) Reducing SnoN expression reverses transformation of A549 and MDA-MB-231 cancer cells. Parental A549 or MDA-MB-231 cells and their derived shSnoN cells were subjected to a soft agar colony assay as described in Materials and Methods. The soft agar plates were stained with 0.5 mg/ml MTT and scanned. A representative 1-cm^2 area of each six-well plate is shown in the top panel. The number of soft agar colonies in each plate was quantified and is summarized in the bottom panel. (B) Reducing SnoN expression blocks tumorigenicity in vivo. Parental or shSnoN-expressing A549 cells were subcutaneously injected into both flanks of five nude mice. A representative nude mouse at 8 weeks after injection with either parental cells or shSnoN cells is shown in the left panel (top). The tumor size of shSnoN-expressing A549 cells was significantly reduced compared with that of the parental A549 tumor (left panel, bottom). The mean tumor volume was calculated as described in Materials and Methods and graphed in the right panel. Each bar represents the mean ± SEM from 10 primary tumors.

itor, SB431542, had no effect on the basal expression of p21, even though this treatment readily blocked TGF-β-induced p21 expression (data not shown). This observation is also consistent with the proposed role of SnoN in maintaining the basal states of some TGF-β-responsive genes. Taken together, these results suggest that reducing SnoN expression in human lung and breast cancer cells enhances cellular responses to TGF-β.

Reducing SnoN expression suppresses tumor growth. TGF-β signaling suppresses tumor growth at early stages of tumorigenesis through its ability to elicit growth arrest (22, 54). Since SnoN represses TGF-β signaling, we reasoned that reducing SnoN expression in cancer cells might diminish or reverse their transformed phenotype. To test this, we first examined the ability of shSnoN-expressing lung and breast cancer cells to undergo anchorage-independent growth in a soft agar assay. Cells were embedded in soft agar and allowed to form colonies for approximately 3 weeks. Under these conditions, parental A549 and MDA-MB-231 cell lines formed colonies readily, whereas cells with reduced expression of SnoN were severely impaired in their growth in soft agar (Fig. 3A). Interestingly, Ski does not appear to play a major role in anchorage-independent growth, since shSki-expressing MDA-MB-231 cells have significantly reduced expression levels of Ski protein yet are still able to form as many soft agar colonies as parental cells do (Fig. 3A, bottom panel). Furthermore, reducing Ski expression in shSnoN-expressing cells did not result in further reduction in soft agar colony formation (data not shown). These results suggest that SnoN but not Ski functions to promote mitogenic transformation.

We next examined whether the decrease in the transforming activity of SnoN-deficient cells in culture resulted in reduced tumorigenicity in vivo. Nude mice were injected with parental cancer cell lines or those lacking SnoN, and tumor number and volume were measured after 8 weeks. Reduction of SnoN expression in lung cancer cells led to a significant decrease in tumor formation, with 40% of shSnoN cell injections leading to tumor formation, compared with 100% of parental A549 cell injections forming tumors (Table 1). Of those SnoN-deficient cells that formed tumors, the average tumor volume was significantly smaller than those formed by parental A549 cells (Fig. 3B and Table 1). Similarly, in nude mice injected with shSnoN-expressing MDA-MB-231 breast cancer cells, a modest but reproducible decrease in tumor number was observed, consistent with the more aggressive and advanced nature of these malignant cells compared with A549 cells (Table 1). As with shSnoN-expressing A549 cells, the tumors that formed from SnoN-deficient MDA-MB-231 cells were significantly smaller (Table 1).

Taken together, our results indicate that SnoN has proncogenic activity and functions to promote tumor growth both in vitro and in vivo.

TABLE 1. Tumorigenicity in athymic nude mice[a]

Cell line	Tumor incidence	Mean tumor vol (cm^3)
A549		
Parental	10/10	1.39 ± 0.53
shSnoN	4/10	0.0875 ± 0.06
MDA-MB-231		
Parental	10/10	2.00 ± 0.49
shSnoN	7/10	0.60 ± 0.52

[a] The indicated cells were grown as described in Materials and Methods. Five mice per cell line were injected subcutaneously in the flank bilaterally. Mice were sacrificed 60 days after injection, and tumor size was measured using hand calipers.

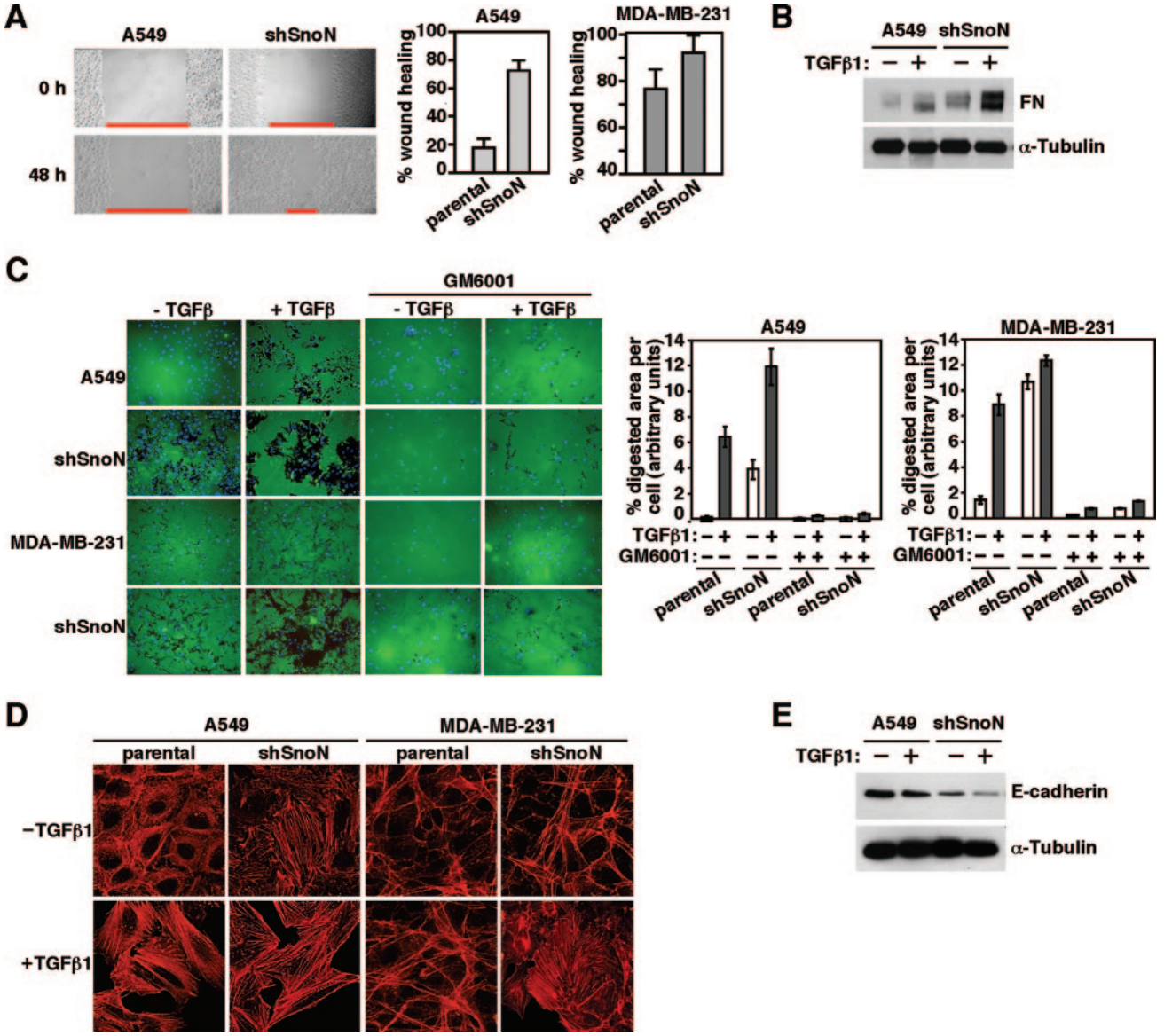

FIG. 4. Reducing SnoN expression enhances EMT. (A) Reducing SnoN expression increases cell motility. Confluent cell monolayers of parental or shSnoN-expressing A549 and MDA-MB-231 cells were wounded with a pipette tip. Wound closure was monitored by microscopy at the indicated times (left panel). Percent wound closure (plotted in right panel) was calculated by measuring the wound closure distance, and this value is expressed as a percentage of the initial wound length. (B) SnoN-deficient A549 cells exhibit increased expression of fibronectin (FN). Parental and shSnoN-expressing A549 cells were treated with 100 pM TGF-β1 for 24 h. Equal amounts of cell lysates prepared from TGF-β-treated and untreated cells were analyzed by Western blotting with antifibronectin. α-Tubulin expression was used as a loading control. (C) Cells expressing shSnoN show increased matrix metalloprotease activity. Parental A549 cells, MDA-MB-231 cells, and their shSnoN-expressing derivatives were cultured on coverslips coated with gelatin-Alexa 488 (to assay MMP2 and MMP9 activity) in the absence or presence of 100 pM TGF-β1 alone or in combination with 10 μM MMP inhibitor GM6001 for 24 to 48 h before processing for immunofluorescence microscopy. Representative in situ zymography micrographs are shown on the left panel. The levels of protease activity within a specified field were quantified by calculating the percentage of digested area normalized to the number of cells within this field and are expressed as the percent digested area per cell (right panel). (D) Reduced expression of SnoN increases stress fiber formation in A549 and MDA-MB-231 cancer cells. Parental A549 cells, MDA-MB-231 cells, and their shSnoN-expressing derivatives were cultured in the absence or presence of 100 pM TGF-β1 for 2 days and then processed for F-actin staining using rhodamine-phalloidin. (E) E-cadherin expression is diminished in SnoN-deficient cells. Parental and shSnoN-expressing A549 cells were treated with 100 pM TGF-β1 for 24 h. Equal amounts of cell lysates prepared from TGF-β-treated and untreated cells were analyzed by Western blotting with anti-E-cadherin. α-Tubulin expression was used as a loading control.

Downregulation of SnoN enhances TGF-β-induced EMT. The EMT is a process by which tumor cells lose epithelial characteristics and acquire the features of mesenchymal cells. It is believed to promote the ability to invade surrounding tissues and blood vessels and undergo metastasis and is thought to be important for malignant progression in vivo. EMT is characterized by a number of morphological and biochemical changes, including increased cell motility and stress

fiber formation, downregulation of adherens junctions and their affiliated proteins, including E-cadherin, induction of extracellular matrix (ECM) proteins, and increased MMP activity (66). Since SnoN potentiates oncogenic transformation and tumor growth, we next asked whether and how SnoN affects the EMT using the A549 and MDA-MB-231 cell lines expressing shSnoN.

We first examined whether expression of SnoN affects the motility of A549 and MDA-MB-231 cells in a wound healing assay. A wound was created by scratching a confluent monolayer of cells with a pipette tip, and relative rates of cell motility were assessed by measuring percent closure of the wound after 48 h of cell migration. Parental A549 cells showed only 18% wound closure within this time period, whereas migration of shSnoN A549 cells resulted in 74% wound closure (Fig. 4A), suggesting that reducing SnoN expression markedly increased cell motility. Similar results were obtained in a transwell migration assay (data not shown). Increased cell motility was also observed in SnoN-deficient MDA-MB-231 breast cancer cells (Fig. 4A, right panel). Since the MDA-MB-231 cells already exhibit a high rate of cell migration, reducing SnoN expression only resulted in a moderate, but reproducible, increase in cell motility. Taken together, these data suggest that SnoN functions to repress cell motility.

Cells that have undergone the EMT also display increased ECM deposition as well as elevated activity of MMPs, for which ECM acts as a substrate. This dynamic production and degradation of ECM is thought to facilitate the movement of tumor cells during metastasis (27, 59). In order to test whether SnoN expression affects induction of ECM proteins, we examined the expression of fibronectin in parental and shSnoN-expressing A549 cells in the absence and presence of TGF-β. TGF-β treatment induced an increase in fibronectin expression in parental lung cancer cells (Fig. 4B). This increase was significantly enhanced in shSnoN cells, suggesting that SnoN normally inhibits induction of fibronectin by TGF-β (Fig. 4B). In situ zymography was employed to examine MMP activity in parental and shSnoN-expressing cells. Cells were plated on fluorescently labeled gelatin, which is a substrate for proteases such as MMP2 and MMP9. Protease activity was assessed by quantifying the degradation of the fluorescently labeled substrates (Fig. 4C). The protease activity was significantly increased in shSnoN-expressing cells relative to parental cells (11.1-fold and 7.5-fold increase in shSnoN A549 cells and MDA-MB-231 cells, respectively) (Fig. 4C, right panels), and this activity was inhibited by the addition of the MMP inhibitor GM6001, suggesting that the protease activity observed was specific to MMPs (Fig. 4C). Treatment with TGF-β stimulated protease activity, as has been reported previously (1, 50, 52), and this TGF-β-induced protease activity was also slightly enhanced in SnoN-deficient tumor cells.

Upon treatment with TGF-β, A549 cells exhibited morphological changes characteristic of EMT, becoming more scattered and elongated, and these TGF-β-induced changes in cell morphology were more pronounced in shSnoN cells (data not shown). Morphological changes occurring during EMT are thought to be due to increased actin stress fibers as well as loss of adherens junctions resulting from downregulation or mislocalization of E-cadherin (27, 49). We therefore examined whether the reduction of SnoN expression affected stress fiber formation by staining cells with fluorescently labeled phalloidin. In parental A549 lung cancer cells and MDA-MB-231 breast cancer cells, cellular actin was arranged cortically, with few or no stress fibers present (Fig. 4D). As has been demonstrated previously in several cell types (9, 10, 51), TGF-β treatment resulted in increased stress fiber formation (Fig. 4D). In shSnoN-expressing lung and breast cancer cells, actin stress fibers were observed even in the absence of TGF-β, and stress fiber formation was further enhanced upon stimulation with TGF-β (Fig. 4D). Thus, downregulation of SnoN in both lung and breast cancer cells augmented actin stress fiber formation.

Loss of adherens junctions due to downregulation or mislocalization of E-cadherin is frequently observed as tumor cells progress to later, more invasive stages of carcinogenesis (49, 60). MDA-MB-231 cells have already lost E-cadherin expression, since they are quite advanced in malignant progression. We therefore examined expression of E-cadherin in parental and shSnoN-expressing A549 cells. TGF-β induced a very slight reduction in E-cadherin levels in parental A549 cells (Fig. 4E). Basal levels of E-cadherin were reduced in shSnoN cells compared with parental A549 cells, and this reduction was more pronounced upon treatment with TGF-β (Fig. 4E), suggesting that downregulation of SnoN promotes disruption of cell-cell contacts. These data are consistent with the morphological observation of enhanced EMT in shSnoN cells.

Taken together, these data indicate that in addition to prooncogenic activity, SnoN also possesses antitumorigenic activity by inhibiting the EMT and possibly tumor metastasis.

Downregulation of SnoN enhances tumor metastasis in vivo. The EMT is thought to play a role in tumor cell metastasis (59). To investigate how SnoN affects tumor cell metastasis, we tested the ability of MDA-MB-231 cells with reduced SnoN expression to form secondary bone and lung metastases in an in vivo metastasis mouse model system. Cells were injected into the left cardiac ventricle of nude mice, and osteolytic bone metastases were quantified after 4 weeks by the histomorphometric measurement of tumor area/burden (in percentage), and metastasis to lung was examined by anatomical analysis of fixed lung tissue at the end of 4 weeks. Interestingly, cells with reduced expression of SnoN appeared to have a moderate but reproducible increase in metastasis to both bone and lung than that of the parental breast cancer cells (Fig. 5A and B). The heightened skeletal metastatic tumor burden in mice inoculated with shSnoN-expressing cells also resulted in severe paraplegia, as evidenced by their diminished latency to fall from a wire hang test (Fig. 5C). Since the formation of metastatic colonies in the in vivo metastasis assay is dependent upon a number of cellular attributes acting in concert, including proliferative potential, migration, and invasion, and in light of the fact that shSnoN cells exhibited significantly reduced proliferative potential, the observation of increased skeletal and lung metastasis may in fact be an under-representation of the migratory and invasive potential of these cells.

We also tested the effects of SnoN on the metastatic potential of lung cancer cells. In this assay, parental A549 lung cancer cells, or the shSnoN-expressing derivatives, were injected into the tail vein of nude mice. If these cells undergo metastasis, they will form secondary tumor modules in the lung that can be identified readily in fixed lung tissues. As shown in Fig. 5D, injection of parental A549 cells resulted in the for-

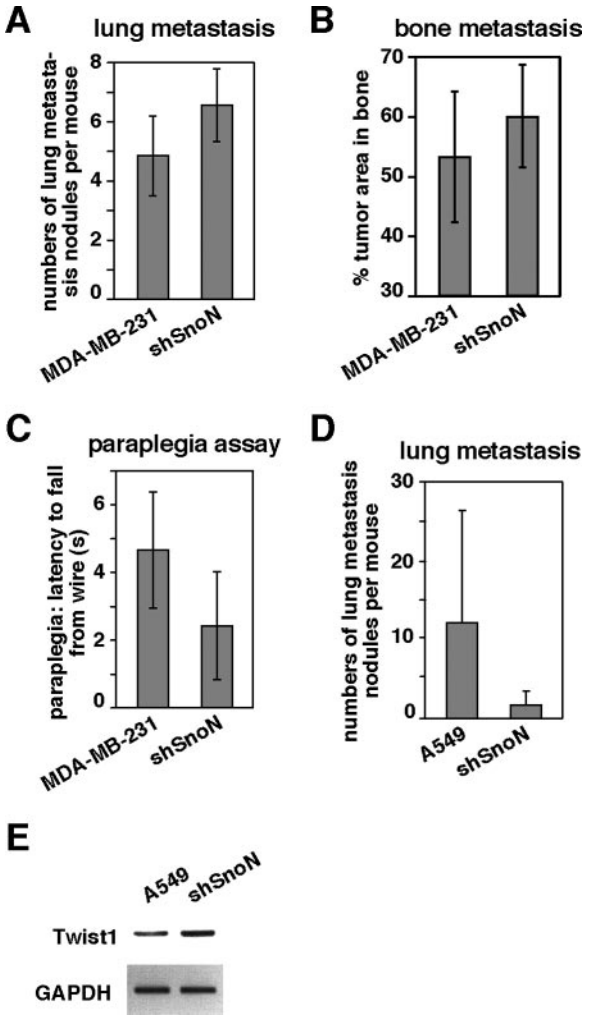

FIG. 5. Effects of downregulation of SnoN on tumor metastasis in vivo. (A) Effects of abrogation of SnoN expression on the lung metastasis of MDA-MB-231 cells. Parental or shSnoN-expressing MDA-MB-231 cells were injected into the left cardiac ventricle of 4-week-old anesthetized female nude mice. Lung metastasis assay was carried out as described in Materials and Methods. The results are expressed as mean ± SEM from eight parental cell-injected mice and seven shSnoN cell-injected mice. (B) Effect of abrogation of SnoN expression on the bone metastasis of MDA-MB-231 cells. The bone metastatic potential is indicated by the histomorphometric measurement of tumor area/burden (in percentage) in the cancellous regions of the right distal femora beginning 100 μm below the growth plates. The area of measurement was 1.5 mm in length, and the width was determined by the inside edges of the cortical bone. The results are expressed as means ± SEM from eight parental cell-injected mice and seven shSnoN cell-injected mice. (C) Paraplegia assay in the parental and shSnoN-expressing MDA-MB-231 cell-injected mice. To detect paraplegia, a wire hang test was performed as described in Materials and Methods. The results are expressed as means ± SEM from six parental cell-injected mice and seven shSnoN cell-injected mice. (D) A549 lung cancer metastasis assay. Parental or shSnoN-expressing A549 cells were injected into the tail veins of 4-week-old female nude mice. After 3 months, 10 mice from each group were euthanized and analyzed as described in Materials and Methods. The number of surface tumor nodules in lungs of each mouse was counted. (E) *Twist1* expression is upregulated in shSnoN-expressing cells. RNA was extracted from parental or shSnoN-expressing A549 cells. An RT-PCR assay was carried out to detect the expression levels of *Twist1* in both parental and shSnoN-expressing A549 cells. RT-PCR with primers amplifying the *GAPDH* locus is shown as a loading control.

mation of extensive lung metastases. In contrast to the results observed in SnoN-deficient breast cancer cells, reducing the level of SnoN expression in lung cancer cells significantly reduced the formation of lung metastases (Fig. 5D). However, it is important to bear in mind that the outcome of these in vivo experiments depends on the combined effects of tumor growth and tumor metastasis. Since the growth of A549 cells is dramatically blocked by a reduction in SnoN expression (Table 1), it is possible that the more pronounced reduction in tumor growth potential in lung cancer cells precluded their ability to form metastatic nodules. In order to bypass the interference of the growth effects and focus on the metastatic potential of these cells, we examined the expression of *Twist1*, a known marker of metastasis, in SnoN-deficient lung cancer cells. In A549 lung cancer cells expressing shSnoN, a modest but reproducible increase in *Twist1* expression was detected (Fig. 5E). This elevation in *Twist1* expression was also confirmed by microarray analysis (see Table 2 and Fig. 8, below). These results are consistent with the increased EMT observed in shSnoN-expressing lung cancer cells and suggest a role for SnoN in inhibiting tumor metastasis.

The effects of SnoN on malignant progression are mediated by both Smad-dependent and Smad-independent mechanisms. In order to confirm the specificity of the results observed in shSnoN cells, we performed "rescue" experiments by reintroducing a wild-type SnoN (WTSnoN) back into the shSnoN-expressing A549 cells and asking whether the reexpressed SnoN reversed the phenotypes of the shSnoN cells. To determine whether the observed effects of SnoN on various aspects of tumorigenesis require its ability to interact with the Smad proteins, a mutant SnoN lacking Smad binding sites (mSnoN) (29, 63) was introduced back into the SnoN-deficient A549 lung cancer cells in parallel with WTSnoN. Both WTSnoN and mSnoN expression constructs contain silent mutations in the *snoN* cDNA that blocks recognition by the *snoN* shRNA. Stable A549 shSnoN clones expressing WTSnoN or mSnoN were generated, and expression of the SnoN proteins was confirmed by Western blotting (Fig. 6A). At least three clones of each were examined in all the biological and biochemical tests, and results from a representative clone are shown. In a growth inhibition assay, reexpression of WTSnoN markedly impaired the ability of shSnoN A549 cells to undergo growth inhibition in response to TGF-β (78% versus 40% growth inhibition, respectively) (Fig. 6B). In contrast, expression of mSnoN did not rescue TGF-β-induced growth arrest (Fig. 6B). This is as expected, since SnoN antagonizes TGF-β signaling through binding to the Smads.

We next tested the ability of WTSnoN to rescue the effects of reducing SnoN on various aspects of malignant transformation. Reexpression of SnoN in shSnoN A549 cells partially restored their ability to undergo anchorage-independent growth (Fig. 6C). The inability of reintroduced SnoN to fully restore oncogenic transformation is mostly likely due to the lower expression level of the ectopically expressed WTSnoN compared with endogenous SnoN in parental A549 cells, as shown in Fig. 6A. Similarly, introduction of WTSnoN mitigated the enhanced EMT responses observed in shShoN-expressing lung cancer cells proportionate to its expression level, as evidenced by the reduced cell motility, the decrease in stress fiber formation, the increase in localization of E-cadherin at

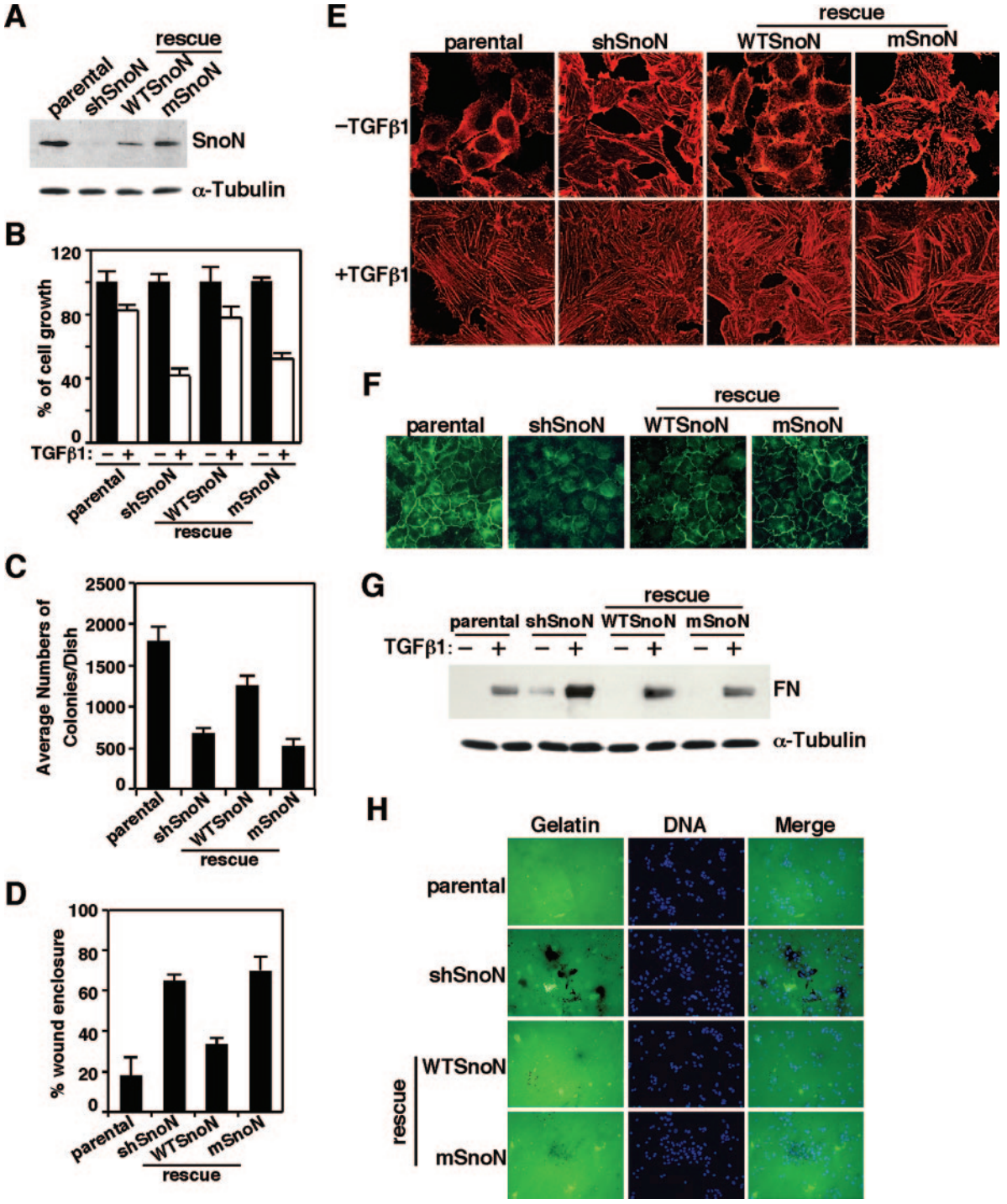

FIG. 6. The effects of SnoN on tumorigenesis are mediated by both Smad-dependent and Smad-independent pathways. (A) Expression levels of wild-type SnoN (WTSnoN) and a mutant SnoN defective in Smad binding (mSnoN) in shSnoN-expressing A549 cells. WTSnoN or mSnoN was stably introduced into shSnoN-expressing A549 cells as described in Materials and Methods. The levels of SnoN protein were assessed by immunoprecipitation and Western blotting with anti-SnoN. The expression levels of α-tubulin in cell lysates are shown as loading controls. (B) TGF-β-elicited growth inhibition in shSnoN A549 cells with reintroduced SnoN proteins. Parental A549 cells, shSnoN-expressing cells, and rescued cells were treated with increasing concentrations of TGF-β1 and cultured for 4 days. The growth of cells was determined by cell counting, and the number is expressed as a percentage of the number of cells in unstimulated samples. (C) Reexpression of SnoN in shSnoN cells partially restores their transformed phenotype. A549 cells, shSnoN cells, and the rescued cells were subjected to a soft agar colony assay as described in Materials and Methods. The number of colonies that formed for each cell type was quantified. (D) Cell motility is reduced upon reexpression of SnoN proteins in shSnoN cells. A wound healing assay was carried out as described in Materials and Methods. (E) Reintroduction of WTSnoN but not mSnoN decreases stress fiber formation in A549 shSnoN-expressing cells. Cells were cultured in the absence or presence of 100 pM TGF-β1 for 2 days and processed for F-actin staining using rhodamine-phalloidin. (F) Introduction of both WT and mutant SnoN restores cell-cell junction E-cadherin expression. Cells were cultured for 2 days to >90% confluence and stained with an anti-E-cadherin antibody. (G) Both WT and mutant SnoN rescue fibronectin expression. Cells were treated with 100 pM TGF-β1 for 24 h. Equal amounts of cell lysates prepared from TGF-β-treated and untreated cells were analyzed by Western blotting with an antifibronectin antibody. α-Tubulin expression was used as a loading control. (H) MMP2 activity is decreased in both rescue cell lines. An in situ zymography assay was carried out as described in Materials and Methods.

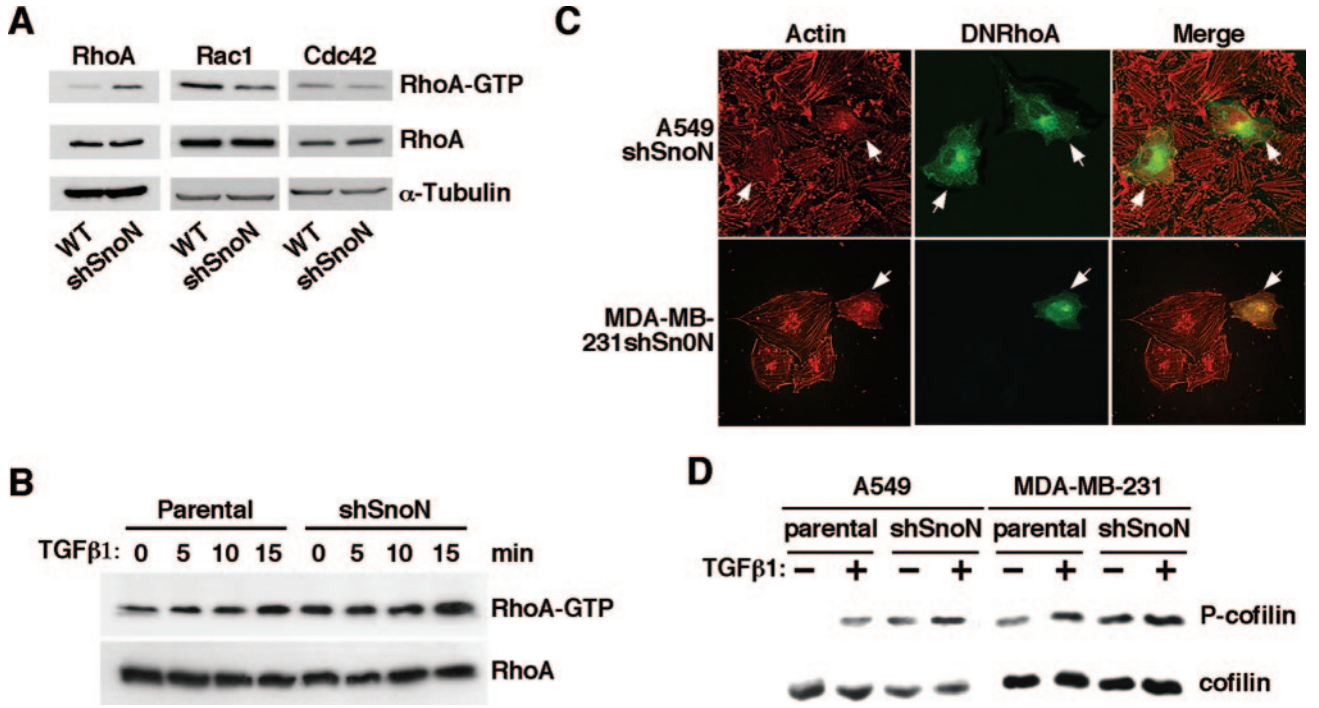

FIG. 7. SnoN inhibits RhoA GTPase activity to block stress fiber formation. (A) Activity of RhoA, not Rac1 or Cdc42, is increased in A549 shSnoN-expressing cells. Equal amounts of cell lysates from parental A549 or shSnoN-expressing cells were subjected to GTPase activity assays as described in Materials and Methods. Total amounts of RhoA, Rac1, or Cdc42 were determined by Western blotting (middle panel). α-Tubulin expression was used as a loading control. (B) TGF-β induces a rapid increase in RhoA activity in both parental and shSnoN-expressing A549 cells. Parental or shSnoN-expressing A549 cells were treated with TGF-β (100 pM) for various times as indicated. RhoA GTPase activity was measured as described in Materials and Methods. (C) Expression of dominant negative RhoA (DNRhoA:T19N) inhibits stress fiber formation in shSnoN-expressing cells. Twenty-four hours after transfection with Myc-RhoA T19N, shSnoN-expressing cells were treated with 100 pM TGF-β1 for 24 h. Myc-RhoA T19N-transfected cells were detected by immunofluorescent staining with anti-Myc (green, white arrowhead). F-actin was stained with rhodamine-phalloidin (red). (D) Phosphorylation of cofilin is enhanced in cells expressing shSnoN. Cells were treated with 100 pM TGF-β1 for 48 h. Equal amounts of cell lysates from TGF-β-treated and untreated cells were analyzed by Western blotting using antibodies against phospho-cofilin (P-cofilin; top panel) or total cofilin (bottom panel).

the cell junction, the decrease in TGF-β-induced fibronectin production, and the decrease in MMP2 activity (Fig. 6D to H). These data confirmed that the phenotypes observed in shSnoN cells are specifically due to the reduction of SnoN expression.

In contrast, introduction of the mutant SnoN defective in binding to the Smad proteins (mSnoN) back into the shSnoN cells failed to restore the anchorage-independent growth (Fig. 6C), even though the expression level of ectopically expressed mSnoN was higher than that of WTSnoN in rescued cells and was comparable to that of endogenous SnoN in parental A549 cells (Fig. 6A). Surprisingly and interestingly, mSnoN can rescue some of the EMT phenotypes found in shSnoN cells, including E-cadherin localization, fibronectin production, and MMP2 activity, but not others, such as stress fiber formation and cell motility (Fig. 6E to H). These data suggest that SnoN inhibits the EMT through both Smad-dependent and Smad-independent pathways and that both pathways are necessary for its effects on malignant progression.

SnoN inhibits RhoA GTPase activity to repress actin stress fiber formation. Since SnoN can activate both Smad-dependent and Smad-independent pathways to regulate EMT, we began to dissect downstream signaling events that may mediate these activities of SnoN. Two approaches were taken. In the first approach, we examined signaling molecules known to regulate various aspects of cell growth, migration, and morphology. In the second approach, microarray analysis was carried out to compare the patterns of gene expression between parental and shSnoN-expressing A549 cells.

The Rho family of small GTPases, including RhoA, Rac, and Cdc42, play important roles in the regulation of cell growth, motility, and actin stress fiber formation (25). Since reducing SnoN expression markedly enhanced actin stress fiber formation, we examined whether SnoN regulates the Rho family of proteins by comparing the expression and activity of RhoA, Rac, and Cdc42 in parental and shSnoN-expressing A549 cells. While SnoN expression had no effect on the expression levels of RhoA, Rac, or Cdc42, the GTP-binding activity of RhoA, but not that of Rac or Cdc42, was significantly elevated in SnoN-deficient cells (Fig. 7A). As reported before (9), TGF-β stimulation resulted in a modest increase in RhoA activity, and this increase was further enhanced in shSnoN cells (Fig. 7B). To determine whether this increase in RhoA activity was required for the enhanced stress fiber formation observed in SnoN-deficient cells, a dominant negative RhoA (DNRhoA:RhoA T19N) was introduced into the shSnoN cells. In untransfected shSnoN A549 or shSnoN MDA-MB-231 cells, actin was arranged in elongated stress fibers as observed previously (Fig. 4D and 7C). In con-

TABLE 2. Selected genes whose expression is altered upon reduction of SnoN expression[a]

Gene function and name	Description	Regulation[b]
Cell growth/proliferation		
CDKN1A (*p21*/*Cip1*)	Cyclin-dependent kinase inhibitor 1A	Up
cyclin G2	Regulation of cyclin-dependent protein kinase activity	Up
JunB	*junB* proto-oncogene, a negative regulator of cell proliferation	Up
IGFBP1	Insulin-like growth factor binding protein 1	Up
GADD34	Negative control of cell growth	Up
GADD45A	Growth arrest and DNA damage inducible, alpha	Up
cyclin E2	Regulation of cyclin-dependent protein kinase activity	Down
cyclin A2	Regulation of cyclin-dependent protein kinase activity	Down
cyclin D3	Regulation of cyclin-dependent protein kinase activity	Down
E2F	Transcription factor, regulation of cell cycle	Down
survivin-β	Negative regulator of caspase 3, 7, and 9	Down
TIAF1	TGFβ1-induced antiapoptotic factor 1	Down
EMT/invasion/metastasis		
Twist1	Twist homolog 1, regulator of EMT	Up
autotaxin	Autocrine motility-stimulating factor (NPP-2), a metastasis-enhancing mitogen	Up
EGFR	Epidermal growth factor receptor, v-*erb* oncogene homolog	Up
VEGF	Vascular endothelial growth factor, regulator of angiogenesis	Up
ORP150	Oxygen-regulated protein, regulator of angiogenesis	Up
ST5	Suppression of tumorigenicity	Up
SEL 1L	Human ortholog of *Caenorhabditis elegans sel-1* gene	Up
TC10	Small Ras-related GTPase	Up
TGFBR3	TGF-β receptor, type III	Down
GDI-1	Rho GDP dissociation inhibitor, alpha	Down
CDKN2C	Cyclin-dependent kinase inhibitor 2C (p18), tumor suppressor	Down
Adhesion/extracellular matrix		
FN1	Fibronectin precursor	Up
ECM2	Extracellular matrix protein 2	Up
integrin α2 β1	Regulator of cell adhesion, migration, and invasion	Up
MMP16	Matrix metalloproteinase 16, activator of MMP2	Up
Decorin	Extracellular matrix component, substrate of MMP16	Up
PLAU	Plasminogen activator, urokinase	Up
Serpine 1/*PAI-1*	Plasminogen activator inhibitor 1	Up
TJP2	Tight junction protein 2	Down
EMP1	Epithelial membrane protein 1	Down

[a] mRNA was isolated from parental A549 and shSnoN-expressing cells and hybridized to Affymetrix GeneChips. Genes whose expression levels significantly increased or decreased in SnoN-deficient cells were sorted into functional groups.
[b] Genes whose signal was increased or decreased in A549 shSnoN cells compared with the levels in parental cells are annotated as "up" or "down," respectively.

trast, cells expressing DNRhoA exhibited diffused cytoplasmic actin staining with no detectable stress fibers (Fig. 7C), suggesting that RhoA activity is required for the increased stress fiber formation observed in SnoN-deficient cells.

Cofilin is an actin-severing protein that is inactivated upon phosphorylation by Lim kinase in a pathway that proceeds downstream of RhoA activation. Phosphorylation and inactivation of cofilin result in stabilization of actin filaments and concomitant stress fiber formation (6). Therefore, increased cofilin phosphorylation is a biochemical marker indicative of increased actin stress fiber formation. In parental lung and breast cancer cells, TGF-β stimulation resulted in phosphorylation of cofilin (Fig. 7D). In cells expressing shSnoN, the basal level of cofilin phosphorylation in untreated cells was heightened relative to parental cells, and TGF-β stimulation further increased the level of cofilin phosphorylation above that observed in TGF-β-treated parental cells (Fig. 7D). This is consistent with the observed increase in RhoA activity and stress fiber formation in these cells.

Taken together, these results indicate that the RhoA pathway appears to function downstream of SnoN to mediate its effect on EMT.

SnoN modulates multiple signaling pathways involved in the regulation of cell growth, migration, and morphology. To further understand the signaling pathways regulated by SnoN and to confirm the biological observations outlined above, we performed microarray analysis to uncover changes in gene expression resulting from downregulation of SnoN expression. Total RNA was isolated from parental A549 cells and those expressing shRNA for SnoN and hybridized to an Affymetrix human U133 (A+B) array. Among the 44,500 total human genes on the array, the expression of 7.8% of them (3,471 genes) was altered upon downregulation of SnoN expression. Out of these 3,471 genes, 2,086 genes were upregulated and 1,348 were downregulated. An annotated list of a subset of these genes is shown in Table 2, and the expression of some of the relevant genes, including *JunB*, *GADD45A*, *EGFR*, *Twist1*, *VEGF*, *PLAU*, and *EMP1* has been confirmed by RT-PCR (Fig. 8).

Consistent with previous data suggesting that SnoN has pleiotropic effects in the regulation of tumorigenesis, SnoN-deficient cells exhibited changes in gene expression indicative of cell cycle arrest as well as EMT leading to tumor metastasis. In particular, several genes involved in negative regulation of

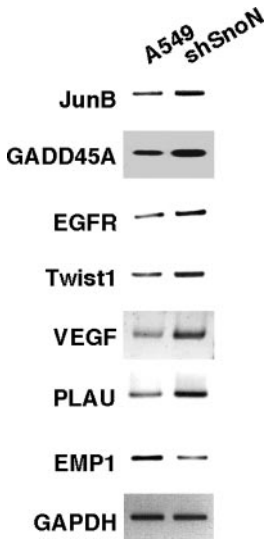

FIG. 8. Alterations in gene expression between parental and SnoN-deficient lung cancer cells. Changes in gene expression for seven loci (*JunB*, *GADD45A*, *EGFR*, *Twist1*, *VEGF*, *PLAU*, and *EMP1*) identified in Table 2 were confirmed by RT-PCR. RT-PCR with primers amplifying the *GAPDH* locus is shown as a loading control.

cell cycle (*p21*, *JunB*, and *cyclin G2*) and apoptosis (*GADD34*, *GADD45*, and *IGFBP1*) were upregulated, while genes that promote cell cycle progression (*cyclin E2*, *A2*, *D3*, and *E2F*) and survival (*survivin-b*) were downregulated in shSnoN cells, in agreement with the reduction of tumor growth both in vitro and in vivo. Many genes involved in extracellular matrix remodeling were induced in SnoN-deficient A549 cells, including *FN1*, *ECM2*, *PLAU*, *PAI-1*, and *MMP-16*. In addition, expression of *Twist1*, an important regulator of EMT that has been shown to promote tumor cell metastasis, was elevated in SnoN-deficient cells. Thus, the ability of SnoN to inhibit cellular processes characteristic of EMT was also substantiated by microarray analysis.

As expected from its role as a negative regulator of TGF-β signaling, many SnoN-regulated genes are also TGF-β-responsive genes. These include several well-described TGF-β-inducible genes (*p21*, *JunB*, *PAI-1*, *cyclin G2*, *MMP2*, *CTGF*, *VEGF*, etc.) that were upregulated in shSnoN cells as well as TGF-β-repressed genes (*cyclin A2*, *TIAF1*, and *TGFβR3*) that were also downregulated in shSnoN cells (7, 15, 19, 31, 34, 37, 39, 43, 46, 47), suggesting that reduction of SnoN expression can enhance or repress expression of TGF-β-regulated genes, even in the absence of TGF-β stimulation (Table 2 and Fig. 2D and 8). This is consistent with a role of SnoN in maintaining the basal states of TGF-β-responsive genes. Not surprisingly, SnoN also altered the expression of many genes not currently known to be directly involved in TGF-β signaling. These include genes involved in cell proliferation and apoptosis (*IGFBP1*, *GADD34*, *E2F*, etc.) and angiogenesis, EMT, and tumor metastasis/invasion (*VEGF*, *SEL1L*, and *autotaxin*) as well as adhesion and cell-matrix interaction (*FN1*, *ECM2*, *α2 integrin*, *MMP2*, *MMP16*, *Decorin*, and *PLAU*) (21, 30, 54). These genes contribute prominently to the complex effects of SnoN on tumor growth and progression.

Taken together, the results of the microarray analysis support cell biological and biochemical observations in SnoN-deficient cells and provide transcriptional data supporting the dual role of SnoN in tumorigenesis.

DISCUSSION

Although high levels of Ski and SnoN can promote oncogenic transformation of chicken embryo fibroblasts in culture (12), the roles of the Ski family of oncoproteins in mammalian carcinogenesis have not been well defined. Adding to the confusion, both protumorigenic and antitumorigenic activities have been attributed to SnoN. To date, transformation of epithelial cells by overexpression of SnoN has not been demonstrated due to technical difficulties inherent in stably expressing high levels of SnoN. In this study, we took the opposite approach to examine the roles of SnoN in mammalian tumorigenesis by a small interfering RNA-mediated reduction of SnoN expression in human cancer cell lines. Using human lung cancer and breast cancer cell lines, we found that SnoN functions to promote mitogenic transformation and tumor growth while inhibiting epithelial-to-mesenchymal transdifferention and tumor metastasis. Human cancer cells with a significantly reduced SnoN expression showed a markedly decreased ability to undergo mitogenic transformation in vitro and tumor growth in vivo (Fig. 3). Interestingly, the same SnoN-deficient cancer cells exhibited increased stress fiber formation, reduced cell contacts, increased motility, and increased expression of extracellular matrix components as well as enhanced matrix metalloproteinase activity, contributing to a more invasive phenotype in vivo (Fig. 4 and 5). Thus, SnoN has dual role in malignant progression; it is protumorigenic at early stages of tumor growth but antitumorigenic at later stages of tumor development. This may have important implications in the design of antitumor treatments targeting SnoN expression. While reducing SnoN expression could reduce tumor size, it may render it more metastatic and thus undermine treatment. Thus, a more specific strategy targeting only the tumor-promoting activity of SnoN is needed.

The proposed dual role of SnoN in transformation lends itself to the hypothesis that the activity of SnoN might be regulated differently during various stages of tumorigenesis. Elevated expression of SnoN may help to establish the primary tumor colonies at the early stages of tumorigenesis by promoting tumor cell growth, by blunting negative regulatory signals such as those elicited by TGF-β, and by limiting the motility of these cells. When the primary tumors have progressed to a stage to spread, SnoN activity may be inhibited either through modification of the SnoN protein or through degradation of the protein, permitting EMT and subsequent metastasis of tumor cells. Once the tumor cells migrate to a new tissue location and are ready to establish secondary colonies, a high level of SnoN expression again will promote tumor growth in the new location. Thus, it is possible that SnoN expression and activity may vary during different stages of malignant progression and that epigenetic or other posttranslational modifications of SnoN may play an important role in the regulation of its activity or expression during malignant progression. While we did not investigate whether there was a correlation between tumor cell invasiveness and reduced SnoN expression among the cancer cell lines analyzed here, it is technically difficult to

accurately compare expression levels of a particular protein among cell types with highly variable cell size and protein contents. In addition, if reduced activity of SnoN is sufficient to promote progression of tumor cells to a more advanced phenotype, this change in SnoN expression may be a transient event and may not be captured by analyzing cancer cell lines derived from tumors with established phenotypes. The possession of antitumor invasion activity by an oncogene product has also been reported to happen to other oncogenes, including Akt1 (33, 36a, 65). Akt1 has been shown to inhibit breast cancer cell motility while promoting the proliferation of these cells. The inhibitory activity of Akt1 on cell motility and invasion appears to be dependent on its ability to activate the E3 ubiquitin ligase HDM2, leading to ubiquitination and degradation of NFAT, an invasion-promoting protein (65). It is possible that other traditionally defined oncoproteins may also play inhibitory roles in EMT, tumor invasion, and metastasis.

The pathways that SnoN activates to regulate oncogenic transformation and EMT are not well understood. One key question related to SnoN function is whether its transforming activity can be fully attributed to its ability to antagonize TGF-β signaling. TGF-β has been shown to inhibit tumor growth at the early stages of tumorigenesis through the Smad-dependent growth inhibitory pathway and to promote EMT and tumor metastasis at late stages through both Smad-dependent and Smad-independent pathways (22, 66). Since SnoN is a negative regulator of the Smad proteins, one would predict that SnoN may operate in the opposite direction as TGF-β during tumorigenesis if these activities are dependent upon its ability to bind to the Smad proteins. Our results suggest that while SnoN indeed has an opposite effect on tumor growth and tumor metastasis as TGF-β, the ability of SnoN to antagonize TGF-β signaling is necessary but not sufficient for its complex roles in tumor development. While many of SnoN-regulated genes are TGF-β-responsive ones and are clearly involved in the regulation of cell proliferation, survival, and EMT, other SnoN target genes that are involved in regulating proliferation and apoptosis, including *E2F*, *GADD34*, and *survivin-b*, as well as a large number of genes involved in EMT, angiogenesis, and metastasis, have not been known to be regulated directly by TGF-β signaling. Although it is possible that some of these genes may not be direct SnoN targets and are instead activated indirectly by primary SnoN-responsive genes, many of them may be regulated directly by SnoN through its ability to affect signaling pathways other than the TGF-β/Smad pathway. One of the pathways regulated by SnoN is the RhoA small GTPase. We showed here that SnoN inhibits the GTPase activity of RhoA and a downstream signaling molecule cofilin to regulate stress fiber formation. Introduction of a dominant negative RhoA blocked stress fiber formation, confirming the importance of RhoA in SnoN signaling. At this time, however, we do not know how SnoN is linked to the activation of RhoA. Microarray analysis showed alterations in the expression of several genes, including Rho GDP dissociation inhibitor alpha and Rho GTPase-activating protein, that could contribute to the activation of RhoA in shSnoN cells. It is also possible that SnoN may inhibit RhoA through a direct signaling cascade independent of its activity as a transcriptional factor. Interestingly, the expression of over 1,000 genes is downregulated in cells lacking SnoN, suggesting that SnoN activity is required for the transcriptional activation of these genes. This could imply that SnoN may function in the capacity of a transcription activator, in addition to acting as a transcriptional corepressor of the Smad proteins. Alternatively, it could be due to an indirect effect of the repressive activity of SnoN: SnoN may inhibit the activity of one or more transcriptional repressors that normally prevent the expression of these genes.

In earlier studies using chicken and quail embryo fibroblasts, Ski and SnoN shared many similarities in their biological activities, including promoting transformation and terminal differentiation. Both proteins bind to the Smad proteins and are potent negative regulators of TGF-β signaling (12, 17, 18, 38, 56, 57, 64). However, it is not clear whether in mammalian cells the two proteins are functionally redundant. Our survey of the various normal and cancerous human cell lines indicated that the two proteins clearly exhibit different patterns of expression. While the expression pattern of SnoN in normal and cancer cells is consistent with its prooncogenic activity, that of Ski is not. Although Ski expression was reported as elevated in malignant melanoma cells in one earlier study (26), a more recent survey of more human melanoma cell lines suggests that most melanoma cell lines may not express detectable level of Ski (48). In addition, we showed that reducing Ski expression had no effect on anchorage-independent growth of breast cancer cells in vitro (Fig. 3A) and tumor growth in vivo (data not shown) but led to increased tumor metastasis (data not shown). Thus, unlike what has been found in chicken embryo fibroblasts that readily undergo anchorage-independent growth in response to Ski overexpression, in mammalian carcinogenesis, Ski may play a role in regulating tumor cell metastasis and invasion rather than tumor growth. Indeed, a recent study by Azuma et al. (5) showed that Ski could inhibit metastasis of a breast cancer cell line to lung and liver. These results raise the important question of whether earlier studies on transformation of chicken embryo fibroblasts by Ski are relevant to human cancer. Future studies hopefully will shed more light on this issue.

ACKNOWLEDGMENTS

We thank X.-F. Wang for the kind gift of the pSuper.retro.puro vector. We acknowledge The Protein and Nucleic Acid Biotechnology Facility at Stanford University, in particular Elizabeth Zuo, for performing the microarray analysis.

This work was supported by NIH grant CA87940 and Philip Morris grant 019016 to K. Luo and NIH grants CA 17542 to G. S. S. Martin and CA79683 to L.-Z. Sun.

REFERENCES

1. **Agarwal, C., J. R. Hembree, E. A. Rorke, and R. L. Eckert.** 1994. Transforming growth factor beta 1 regulation of metalloproteinase production in cultured human cervical epithelial cells. Cancer Res **54:**943–949.
2. **Akhurst, R. J., and R. Derynck.** 2001. TGF-beta signaling in cancer—a double-edged sword. Trends Cell Biol. **11:**S44–S51.
3. **Akiyoshi, S., H. Inoue, J. Hanai, K. Kusanagi, N. Nemoto, K. Miyazono, and M. Kawabata.** 1999. c-Ski acts as a transcriptional co-repressor in transforming growth factor-beta signaling through interaction with smads. J. Biol. Chem. **274:**35269–35277.
4. **Attisano, L., and J. L. Wrana.** 2002. Signal transduction by the TGF-beta superfamily. Science **296:**1646–1647.
5. **Azuma, H., S. Ehata, H. Miyazaki, T. Watabe, O. Maruyama, T. Imamura, T. Sakamoto, S. Kiyama, Y. Kiyama, T. Ubai, T. Inamoto, S. Takahara, Y. Itoh, Y. Otsuki, Y. Katsuoka, K. Miyazono, and S. Horie.** 2005. Effect of Smad7 expression on metastasis of mouse mammary carcinoma JygMC(A) cells. J. Natl. Cancer Inst **97:**1734–1746.
6. **Bamburg, J. R.** 1999. Proteins of the ADF/cofilin family: essential regulators of actin dynamics. Annu. Rev. Cell Dev. Biol. **15:**185–230.
7. **Barlat, I., B. Henglein, A. Plet, N. Lamb, A. Fernandez, F. McKenzie, J.**

Pouyssegur, A. Vie, and J. M. Blanchard. 1995. TGF-beta 1 and cAMP attenuate cyclin A gene transcription via a cAMP responsive element through independent pathways. Oncogene **11:**1309–1318.
8. **Berdeaux, R. L., B. Diaz, L. Kim, and G. S. Martin.** 2004. Active Rho is localized to podosomes induced by oncogenic Src and is required for their assembly and function. J. Cell Biol. **166:**317–323.
9. **Bhowmick, N. A., M. Ghiassi, A. Bakin, M. Aakre, C. A. Lundquist, M. E. Engel, C. L. Arteaga, and H. L. Moses.** 2001. Transforming growth factor-β1 mediates epithelial to mesenchymal transdifferentiation through a RhoA-dependent mechanism. Mol. Biol. Cell **12:**27–36.
10. **Boland, S., E. Boisvieux-Ulrich, O. Houcine, A. Baeza-Squiban, M. Pouchelet, D. Schoevaert, and F. Marano.** 1996. TGF beta 1 promotes actin cytoskeleton reorganization and migratory phenotype in epithelial tracheal cells in primary culture. J. Cell Sci. **109:**2207–2219.
11. **Bonni, S., H. R. Wang, C. G. Causing, P. Kavsak, S. L. Stroschein, K. Luo, and J. L. Wrana.** 2001. TGF-beta induces assembly of a Smad2-Smurf2 ubiquitin ligase complex that targets SnoN for degradation. Nat. Cell Biol. **3:**587–595.
12. **Boyer, P. L., C. Colmenares, E. Stavnezer, and S. H. Hughes.** 1993. Sequence and biological activity of chicken snoN cDNA clones. Oncogene **8:**457–466.
13. **Briand, P., O. W. Petersen, and B. van Deurs.** 1987. A new diploid nontumorigenic human breast epithelial cell line isolated and propagated in chemically defined medium. In Vitro Cell Dev. Biol. **23:**181–188.
14. **Brummelkamp, T. R., R. Bernards, and R. Agami.** 2002. A system for stable expression of short interfering RNAs in mammalian cells. Science **296:**550–553.
15. **Chang, N. S., J. Mattison, H. Cao, N. Pratt, Y. Zhao, and C. Lee.** 1998. Cloning and characterization of a novel transforming growth factor-beta1-induced TIAF1 protein that inhibits tumor necrosis factor cytotoxicity. Biochem. Biophys. Res. Commun. **253:**743–749.
16. **Cohen, S. B., R. Nicol, and E. Stavnezer.** 1998. A domain necessary for the transforming activity of SnoN is required for specific DNA binding, transcriptional repression and interaction with TAF(II)110. Oncogene **17:**2505–2513.
17. **Colmenares, C., and E. Stavnezer.** 1989. The ski oncogene induces muscle differentiation in quail embryo cells. Cell **59:**293–303.
18. **Colmenares, C., P. Sutrave, S. H. Hughes, and E. Stavnezer.** 1991. Activation of the c-*ski* oncogene by overexpression. J. Virol. **65:**4929–4935.
19. **Datto, M. B., Y. Li, J. F. Panus, D. J. Howe, Y. Xiong, and X. F. Wang.** 1995. Transforming growth factor β induces the cyclin-dependent kinase inhibitor p21 through a p53-independent mechanism. Proc. Natl. Acad. Sci. USA **92:**5545–5549.
20. **Debnath, J., S. K. Muthuswamy, and J. S. Brugge.** 2003. Morphogenesis and oncogenesis of MCF-10A mammary epithelial acini grown in three-dimensional basement membrane cultures. Methods **30:**256–268.
21. **DeClerck, Y. A., A. M. Mercurio, M. S. Stack, H. A. Chapman, M. M. Zutter, R. J. Muschel, A. Raz, L. M. Matrisian, B. F. Sloane, A. Noel, M. J. Hendrix, L. Coussens, and M. Padarathsingh.** 2004. Proteases, extracellular matrix, and cancer: a workshop of the path B study section. Am. J. Pathol. **164:**1131–1139.
22. **Derynck, R., R. J. Akhurst, and A. Balmain.** 2001. TGF-beta signaling in tumor suppression and cancer progression. Nat. Genet. **29:**117–129.
23. **Derynck, R., and Y. E. Zhang.** 2003. Smad-dependent and Smad-independent pathways in TGF-beta family signalling. Nature **425:**577–584.
24. **Edmiston, J. S., W. A. Yeudall, T. D. Chung, and D. A. Lebman.** 2005. Inability of transforming growth factor-beta to cause SnoN degradation leads to resistance to transforming growth factor-beta-induced growth arrest in esophageal cancer cells. Cancer Res **65:**4782–4788.
25. **Etienne-Manneville, S., and A. Hall.** 2002. Rho GTPases in cell biology. Nature **420:**629–635.
26. **Fumagalli, S., L. Doneda, N. Nomura, and L. Larizza.** 1993. Expression of the c-ski proto-oncogene in human melanoma cell lines. Melanoma Res. **3:**23–27.
27. **Grunert, S., M. Jechlinger, and H. Beug.** 2003. Diverse cellular and molecular mechanisms contribute to epithelial plasticity and metastasis. Nat. Rev. Mol. Cell Biol. **4:**657–665.
28. **Hattori, K., H. Lee, P. D. Hurn, B. J. Crain, R. J. Traystman, and A. C. DeVries.** 2000. Cognitive deficits after focal cerebral ischemia in mice. Stroke **31:**1939–1944.
29. **He, J., S. B. Tegen, A. R. Krawitz, G. S. Martin, and K. Luo.** 2003. The transforming activity of Ski and SnoN is dependent on their ability to repress the activity of Smad proteins. J. Biol. Chem. **278:**30540–30547.
30. **Heissig, B., K. Hattori, M. Friedrich, S. Rafii, and Z. Werb.** 2003. Angiogenesis: vascular remodeling of the extracellular matrix involves metalloproteinases. Curr. Opin. Hematol. **10:**136–141.
31. **Horne, M. C., K. L. Donaldson, G. L. Goolsby, D. Tran, M. Mulheisen, J. W. Hell, and A. F. Wahl.** 1997. Cyclin G2 is up-regulated during growth inhibition and B cell antigen receptor-mediated cell cycle arrest. J. Biol. Chem. **272:**12650–12661.
32. **Imoto, I., A. Pimkhaokham, Y. Fukuda, Z. Q. Yang, Y. Shimada, N. Nomura, H. Hirai, M. Imamura, and J. Inazawa.** 2001. SNO is a probable target for gene amplification at 3q26 in squamous-cell carcinomas of the esophagus. Biochem. Biophys. Res. Commun. **286:**559–565.
33. **Irie, H. Y., R. V. Pearline, D. Grueneberg, M. Hsia, P. Ravichandran, N. Kothari, S. Natesan, and J. S. Brugge.** 2005. Distinct roles of Akt1 and Akt2 in regulating cell migration and epithelial-mesenchymal transition. J. Cell Biol. **171:**1023–1034.
34. **Keeton, M. R., S. A. Curriden, A. J. van Zonneveld, and D. J. Loskutoff.** 1991. Identification of regulatory sequences in the type 1 plasminogen activator inhibitor gene responsive to transforming growth factor beta. J. Biol. Chem. **266:**23048–23052.
35. **Kokura, K., S. C. Kaul, R. Wadhwa, T. Nomura, M. M. Khan, T. Shinagawa, T. Yasukawa, C. Colmenares, and S. Ishii.** 2001. The Ski protein family is required for MeCP2-mediated transcriptional repression. J. Biol. Chem. **276:**34115–34121.
36. **Krakowski, A. R., J. Laboureau, A. Mauviel, M. J. Bissell, and K. Luo.** 2005. Cytoplasmic SnoN in normal tissues and nonmalignant cells antagonizes TGF-beta signaling by sequestration of the Smad proteins. Proc. Natl. Acad. Sci. USA **102:**12437–12442.
36a. **Liu, H., D. C. Radisky, C. M. Nelson, H. Zhang, J. E. Fata, R. A. Roth, and M. J. Bissell.** 2006. Mechanism of Akt1 initiation of breast cancer invasion reveals a protumorigenic role for TSC 2. Proc. Natl. Acad. Sci. USA **103:**4134–4139.
37. **Lopez-Casillas, F., C. Riquelme, Y. Perez-Kato, M. V. Ponce-Castaneda, N. Osses, J. Esparza-Lopez, G. Gonzalez-Nunez, C. Cabello-Verrugio, V. Mendoza, V. Troncoso, and E. Brandan.** 2003. β-Glycan expression is transcriptionally up-regulated during skeletal muscle differentiation. Cloning of murine betaglycan gene promoter and its modulation by MyoD, retinoic acid, and transforming growth factor-beta. J. Biol. Chem. **278:**382–390.
38. **Luo, K., S. L. Stroschein, W. Wang, D. Chen, E. Martens, S. Zhou, and Q. Zhou.** 1999. The Ski oncoprotein interacts with the Smad proteins to repress TGFβ signaling. Genes Dev. **13:**2196–2206.
39. **Ma, C., R. W. Tarnuzzer, and N. Chegini.** 1999. Expression of matrix metalloproteinases and tissue inhibitor of matrix metalloproteinases in mesothelial cells and their regulation by transforming growth factor-beta1. Wound Repair Regen. **7:**477–485.
40. **Massague, J., and D. Wotton.** 2000. Transcriptional control by the TGF-beta/Smad signaling system. EMBO J. **19:**1745–1754.
41. **Moustakas, A., K. Pardali, A. Gaal, and C. H. Heldin.** 2002. Mechanisms of TGF-beta signaling in regulation of cell growth and differentiation. Immunol. Lett. **82:**85–91.
42. **Nomura, N., S. Sasamoto, S. Ishii, T. Date, M. Matsui, and R. Ishizaki.** 1989. Isolation of human cDNA clones of ski and the ski-related gene, sno. Nucleic Acids Res. **17:**5489–5500.
43. **Oemar, B. S., A. Werner, J. M. Garnier, D. D. Do, N. Godoy, M. Nauck, W. Marz, J. Rupp, M. Pech, and T. F. Luscher.** 1997. Human connective tissue growth factor is expressed in advanced atherosclerotic lesions. Circulation **95:**831–839.
44. **Pearson-White, S.** 1993. SnoI, a novel alternatively spliced isoform of the ski protooncogene homolog, sno. Nucleic Acids Res. **21:**4632–4638.
45. **Pearson-White, S., and R. Crittenden.** 1997. Proto-oncogene Sno expression, alternative isoforms and immediate early serum response. Nucleic Acids Res. **25:**2930–2937.
46. **Pertovaara, L., A. Kaipainen, T. Mustonen, A. Orpana, N. Ferrara, O. Saksela, and K. Alitalo.** 1994. Vascular endothelial growth factor is induced in response to transforming growth factor-beta in fibroblastic and epithelial cells. J. Biol. Chem. **269:**6271–6274.
47. **Pertovaara, L., L. Sistonen, T. J. Bos, P. K. Vogt, J. Keski-Oja, and K. Alitalo.** 1989. Enhanced *jun* gene expression is an early genomic response to transforming growth factor β stimulation. Mol. Cell. Biol. **9:**1255–1262.
48. **Poser, I., T. Rothhammer, S. Dooley, R. Weiskirchen, and A. K. Bosserhoff.** 2005. Characterization of Sno expression in malignant melanoma. Int. J. Oncol. **26:**1411–1417.
49. **Savagner, P.** 2001. Leaving the neighborhood: molecular mechanisms involved during epithelial-mesenchymal transition. Bioessays **23:**912–923.
50. **Sehgal, I., and T. C. Thompson.** 1999. Novel regulation of type IV collagenase (matrix metalloproteinase-9 and -2) activities by transforming growth factor-beta1 in human prostate cancer cell lines. Mol. Biol. Cell **10:**407–416.
51. **Shen, X., J. Li, P. P. Hu, D. Waddell, J. Zhang, and X. F. Wang.** 2001. The activity of guanine exchange factor NET1 is essential for transforming growth factor-beta-mediated stress fiber formation. J. Biol. Chem. **276:**15362–15368.
52. **Shimizu, S., Y. Nishikawa, K. Kuroda, S. Takagi, K. Kozaki, S. Hyuga, S. Saga, and M. Matsuyama.** 1996. Involvement of transforming growth factor beta1 in autocrine enhancement of gelatinase B secretion by murine metastatic colon carcinoma cells. Cancer Res **56:**3366–3370.
53. **Shinagawa, T., H.-D. Dong, M. Xu, T. Maekawa, and S. Ishii.** 2000. The sno gene, which encodes a component of the histone deacetylation complex, acts as a tumor suppressor in mice. EMBO J. **19:**2280–2291.
54. **Siegel, P. M., and J. Massague.** 2003. Cytostatic and apoptotic actions of TGF-beta in homeostasis and cancer. Nat. Rev. Cancer **3:**807–821.
55. **Stroschein, S. L., S. Bonni, J. L. Wrana, and K. Luo.** 2001. Smad3 recruits the anaphase-promoting complex for ubiquitination and degradation of SnoN. Genes Dev. **15:**2822–2836.

56. **Stroschein, S. L., W. Wang, S. Zhou, Q. Zhou, and K. Luo.** 1999. Negative feedback regulation of TGF-beta signaling by the SnoN oncoprotein. Science **286:**771–774.
57. **Sun, Y., X. Liu, E. N. Eaton, W. S. Lane, H. F. Lodish, and R. A. Weinberg.** 1999. Interaction of the Ski oncoprotein with Smad3 regulates TGF-beta signaling. Mol. Cell **4:**499–509.
58. **Sun, Y., X. Liu, E. Ng-Eaton, H. F. Lodish, and R. A. Weinberg.** 1999. SnoN and Ski protooncoproteins are rapidly degraded in response to transforming growth factor beta signaling. Proc. Natl. Acad. Sci. USA **96:**12442–12447.
59. **Thiery, J. P.** 2002. Epithelial-mesenchymal transitions in tumour progression. Nat. Rev. Cancer **2:**442–454.
60. **Thiery, J. P., and D. Chopin.** 1999. Epithelial cell plasticity in development and tumor progression. Cancer Metastasis Rev. **18:**31–42.
61. **Wakefield, L. M., and A. B. Roberts.** 2002. TGF-beta signaling: positive and negative effects on tumorigenesis. Curr. Opin. Genet. Dev. **12:**22–29.
62. **Wilkinson, D. S., S. K. Ogden, S. A. Stratton, J. L. Piechan, T. T. Nguyen, G. A. Smulian, and M. C. Barton.** 2005. A direct intersection between p53 and transforming growth factor beta pathways targets chromatin modification and transcription repression of the alpha-fetoprotein gene. Mol. Cell. Biol. **25:**1200–1212.
63. **Wu, J. W., A. R. Krawitz, J. Chai, W. Li, F. Zhang, K. Luo, and Y. Shi.** 2002. Structural mechanism of Smad4 recognition by the nuclear oncoprotein Ski: insights on Ski-mediated repression of TGF-beta signaling. Cell **111:**357–367.
64. **Xu, W., K. Angelis, D. Danielpour, M. M. Haddad, O. Bischof, J. Campisi, E. Stavnezer, and E. E. Medrano.** 2000. Ski acts as a co-repressor with Smad2 and Smad3 to regulate the response to type beta transforming growth factor. Proc. Natl. Acad. Sci. USA **97:**5924–5929.
65. **Yoeli-Lerner, M., G. K. Yiu, I. Rabinovitz, P. Erhardt, S. Jauliac, and A. Toker.** 2005. Akt blocks breast cancer cell motility and invasion through the transcription factor NFAT. Mol. Cell **20:**539–550.
66. **Zavadil, J., and E. P. Bottinger.** 2005. TGF-beta and epithelial-to-mesenchymal transitions. Oncogene **24:**5764–5774.
67. **Zhang, F., M. Lundin, A. Ristimaki, P. Heikkila, J. Lundin, J. Isola, H. Joensuu, and M. Laiho.** 2003. Ski-related novel protein N (SnoN), a negative controller of transforming growth factor-beta signaling, is a prognostic marker in estrogen receptor-positive breast carcinomas. Cancer Res **63:**5005–5010.
68. **Zhu, Q., S. Pearson-White, and K. Luo.** 2005. Requirement for the SnoN oncoprotein in transforming growth factor beta-induced oncogenic transformation of fibroblast cells. Mol. Cell. Biol. **25:**10731–10744.